

von **KARMAN INSTITUTE**
FOR FLUID DYNAMICS

TECHNICAL NOTE 67 TECHNISCHE HOGESCHOOL
VLIEGTUIGBOUWKUNDE
BIBLIOTHEEK

COMPRESSIBLE BOUNDARY LAYER FLOW PAST 2 APR. 1971
A SWEPT WAVY WALL WITH HEAT
TRANSFER AND ABLATION

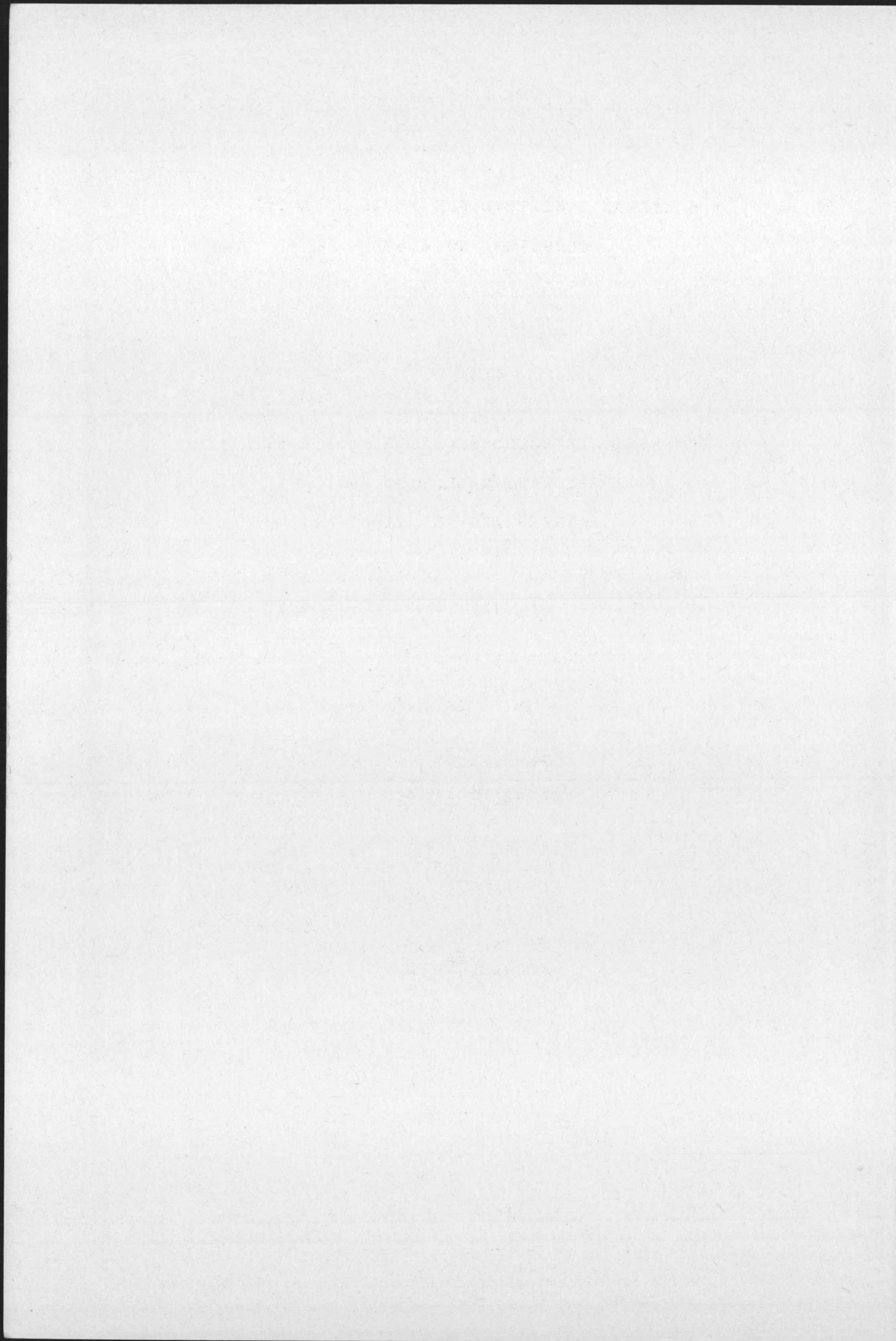
by

G. R. INGER
Visiting Professor



RHODE-SAINT-GENESE, BELGIUM

DECEMBER 1970



VON KARMAN INSTITUTE FOR FLUID DYNAMICS

TECHNICAL NOTE 67

COMPRESSIBLE BOUNDARY LAYER FLOW PAST

A SWEEPED WAVY WALL WITH HEAT

TRANSFER AND ABLATION

by

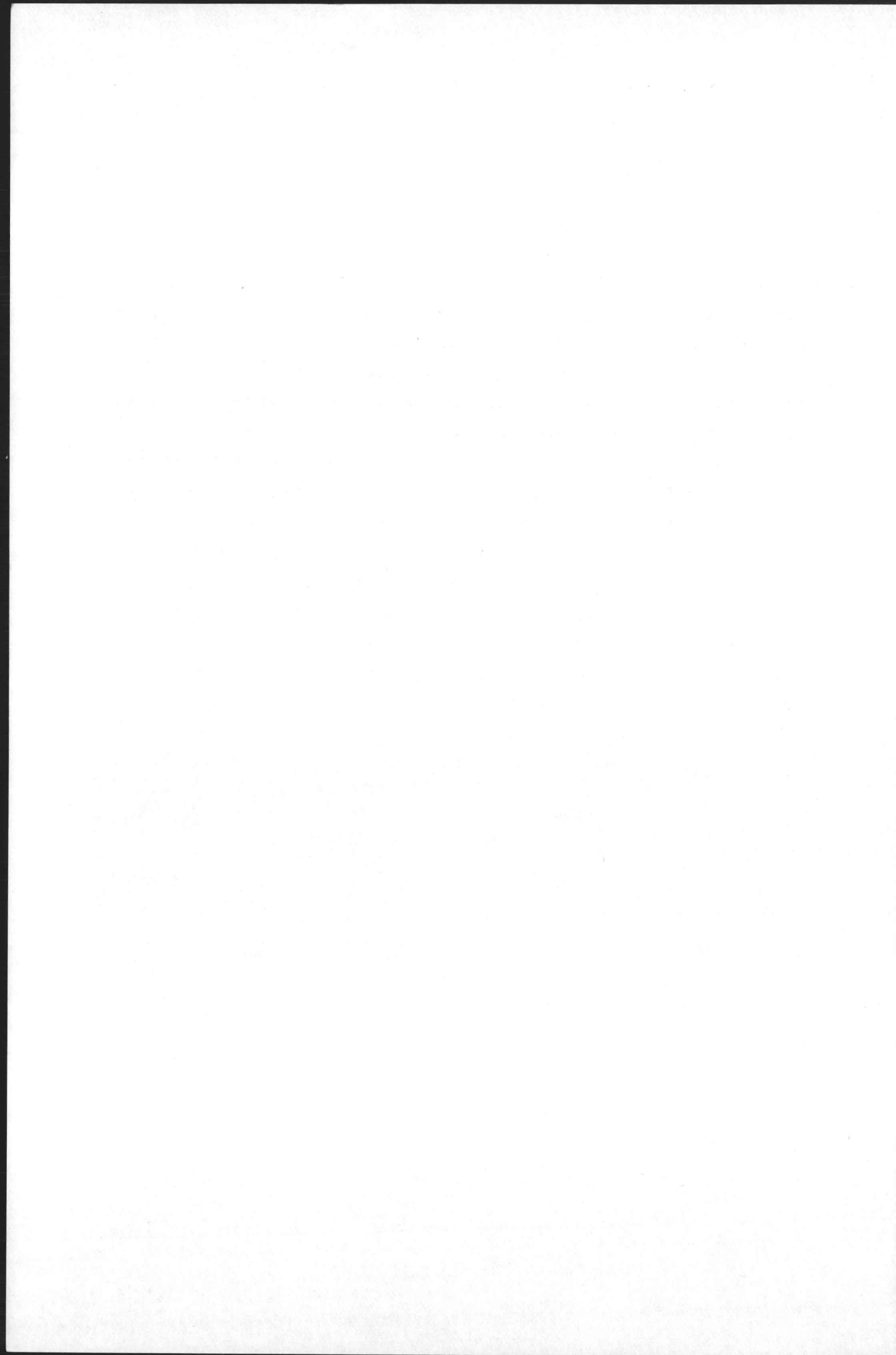
G. R. INGER

Visiting Professor

DECEMBER 1970

ABSTRACT

Steady small disturbances in a compressible boundary layer flow past a slightly wavy swept wall are analyzed including the effects of compressibility, heat transfer and possible ablative response of the wall surface. The theory indicates that the non-uniform flow in the boundary layer can produce a subsonic wall pressure signature even when the local inviscid flow is moderately supersonic. For an ablating surface at high heat transfer rates, it is shown that the interaction of the gas dynamic and surface material disturbances can lead to a condition of "resonance" at a certain critical ratio of boundary layer thickness to surface wavelength. The results of some recent wind tunnel studies of turbulent boundary layer flows past a nonablating wavy wall in the Mach number range $.8 \leq M_e \leq 1.8$ are also shown to corroborate theoretical predictions of both pressure and temperature perturbations.



1. INTRODUCTION

This paper describes a study of the gas dynamic disturbances within compressible boundary layer flow past a slightly wave swept wall including the effects of surface ablation. The results find practical application in engineering studies of surface disturbance effects on high speed boundary layer separation and heating (ref. 1, 2), panel flutter (ref.3), hydrodynamic stability of compressible boundary layers on deformable surfaces (ref. 4) and ablation surface cross-hatching (ref. 5). Since in practice the boundary layer along the wavy surface is often turbulent, the present investigation is mainly concerned with this case although the theoretical results can also be applied equally well to laminar flows.

In Section 2, an approximate linearized theory of compressible non-uniform flow past a slightly wavy wall is presented, including the temperature, heat and mass transfer perturbation aspects of the flow. In particular, the analysis contains significant extensions of previous work on the viscous sublayer to include compressibility and heat transfer effects. In Section 3, the corresponding disturbances within the wall material are analyzed when the wavy wall is a rapidly ablating pure sublimator. It is shown that the mutual interaction between the boundary layer gas dynamic disturbances and these ablative perturbations can lead to a condition of "resonance" between them. Section 4 presents a comparison of the present theory with some recent wind tunnel measurements (ref. 6) of pressure and temperature disturbances on a non-ablating wavy wall. Finally, in Section 5 the major results of this study are summarized and areas for further investigation are discussed briefly.

2. THEORETICAL ANALYSIS

The analysis is based on an equivalent inviscid flow model of the mean (undisturbed) boundary layer and a linearized small disturbance treatment of the perturbation field in which the solution is linearly decomposed into a "slowly-varying" inviscid part which determines the pressure and a "rapidly-varying" viscous part that is important near the wall. The pressure field is analyzed first using an approach similar to one developed some years ago by Lighthill (ref. 7). Some interesting thermodynamic aspects of the inviscid disturbance field are observed from this analysis. The additional effects of viscosity and heat conduction are then considered, again on the basis of extending some work by Lighthill on viscous sublayer effects in perturbed boundary layer flows (ref. 8). The surface shear and heat transfer perturbations are determined by this analysis for solid surfaces with either fixed temperature or heat transfer and also for a surface undergoing quasi-steady ablation due to large heat transfer from the adjacent boundary layer.

2.1 General considerations

We assume steady compressible boundary layer flow of a perfect gas with unit Prandtl and Lewis numbers, subjected to steady perturbations sufficiently small that they may be treated by linearized theory (transonic or hypersonic mean flows are thereby excluded). Following the arguments of Lighthill (ref. 7) and Benjamin (ref. 9), the mean flow is idealized in the first approximation as a rotational plane parallel shear flow in the x -direction with uniform static pressure p_∞ and arbitrary variations of density $\rho_0(y)$, velocity $U_0(y)$, Mach number $M_0(y)$ and temperature $T_0(y)$ in the normal (y) direction. The steady perturbations are taken to be caused by a stationary rippled surface $y_w(x) = \epsilon \sin \alpha$ lying in the x - z plane as schematically illustrated in Fig. 1, where $\xi = x \sin \phi - z \cos \phi$ is the coordinate perpendicular to the crests, ϕ the sweep angle of the ripple pattern (here taken as arbitrary), ϵ the

amplitude and $\alpha = \frac{2\pi}{\lambda}$ the reciprocal wave length.

Each of the total flow properties is expressed as the sum of the mean value and a small perturbation harmonic in $\alpha\xi$; denoting $E \equiv \exp(i\alpha\xi)$ we thus write

$$U = U_0(y) + E \tilde{U}(y)$$

$$V = E \tilde{V}(y)$$

$$W = E \tilde{W}(y)$$

$$p = p_\infty + E \tilde{P}(y)$$

$$\rho = \rho_0(y) + E \tilde{R}(y)$$

$$T = T_0(y) + E \tilde{T}(y)$$

where it is understood that only the real parts of these generally-complex quantities are of ultimate physical interest. In addition, we introduce the following velocity variables resolved in the ξ -direction:

$$q_0 = U_0 \sin\phi$$

$$\tilde{Q} = \tilde{U} \sin\phi - \tilde{W} \cos\phi$$

$$W^* = \tilde{W} \sec\phi$$

Then substituting these expressions into the general compressible Navier-Stokes equations, applying the aforementioned simplifying assumptions, retaining only first order perturbations and in the case of turbulent flow making the assumption of quasi-laminar behavior in the perturbation field (ref. 10), one finally obtains the following set of ordinary differential equations governing the perturbation distribution functions \tilde{Q} , \tilde{V} , \tilde{P} , etc:

$$i\alpha(\rho_0 Q + q_0 \tilde{R}) + \frac{d}{dy} (\rho_0 \tilde{V}) = 0 \quad (1)$$

$$\left. \begin{aligned} i\alpha\rho_0 q_0 \tilde{Q} + \rho_0 \frac{dq_0}{dy} \tilde{V} + i\alpha\tilde{P} &= \frac{d}{dy} (\mu_0 (\frac{d\tilde{Q}}{dy} + i\alpha\tilde{V})) \\ + \frac{d}{dy} (\tilde{\mu} \frac{dq_0}{dy}) - \frac{2}{3} \mu_0 (i\alpha \frac{d\tilde{V}}{dy} + 2\tilde{Q}\alpha^2) \end{aligned} \right\} \quad (2)$$

$$\left. \begin{aligned} i\alpha\rho_0 q_0 \tilde{V} + \frac{d\tilde{P}}{dy} &= \frac{4}{3} \frac{d}{dy} (\mu_0 (\frac{d\tilde{V}}{dy} - \frac{i\alpha}{2} \tilde{Q})) \\ + i\alpha \frac{dq_0}{dy} \tilde{\mu} + \mu_0 (i\alpha \frac{d\tilde{Q}}{dy} - \alpha^2 \tilde{V}) \end{aligned} \right\} \quad (3)$$

$$\left. \begin{aligned} i\alpha\rho_0 q_0 \tilde{H} + \rho_0 \frac{dH_0}{dy} \tilde{V} &= \frac{d}{dy} (\mu_0 (\frac{d\tilde{H}}{dy} + i\alpha q_0 \tilde{V})) + \tilde{\mu} \frac{dH_0}{dy} \\ + i\alpha\mu_0 \frac{dq_0}{dy} - \tilde{U} \csc\phi \frac{d}{dy} (\mu_0 \frac{dq_0}{dy}) \\ - \mu_0 \alpha^2 (\tilde{H} + \frac{1}{3} q_0 \tilde{Q} + \frac{2}{3} \cos\phi q_0 \tilde{V}) \end{aligned} \right\} \quad (4)$$

$$\tilde{R} = \rho_0 \left(\frac{\tilde{P}}{p_\infty} - \frac{\tilde{T}}{T_0} \right) \quad (5)$$

$$i\alpha\rho_0 q_0 W^* - i\alpha\tilde{P} = \frac{d}{dy} (\mu_0 (\frac{dW^*}{dy} - i\alpha\tilde{V})) + \mu_0 \left(\frac{2}{3} i\alpha \frac{d\tilde{V}}{dy} - \alpha^2 (W^* - \frac{1}{3} \tilde{Q}) \right) \quad (6)$$

where μ_0 and $\tilde{\mu}$ are the mean and perturbation effective viscosities, respectively, and where the energy equation (4) has been written in terms of the mean total enthalpy $H_0 = C_p T_0 + (U_0^2/2)$ and its perturbation $\tilde{H} = C_p \tilde{T} + U_0 \tilde{U} = C_p \tilde{T} + q_0 \tilde{U} \cos\phi$.

Now it can be seen that if the effects of viscous dissipation heating on the temperature field (as represented

by the last two terms of eq. 4) are neglected, the foregoing equations become independent of the wavy wall sweep angle ϕ and the parallel mean flow approximation has thus resulted in reducing the original three-dimensional disturbance problem to an equivalent two-dimensional one in the direction normal to the surface waves. Correspondingly, it is noted that this resolved perturbation problem is independent of the lateral velocity variable W^* , which can be subsequently found from eq. 6 after the other equations are first solved. Both Lees and Reshotko (ref. 11) and Brown (ref. 12) have shown that the parallel flow and negligible viscous dissipation approximations are acceptable at moderate supersonic speeds but can break down in strongly hypersonic boundary layers.

The formulation is completed by a specification of the boundary conditions. Consider first the outer edge $y = \delta$ of the boundary layer where the mean flow gradients vanish. Here the viscous effects on the perturbation field are taken to vanish exponentially (ref. 11) while the remaining inviscid solutions are assumed to be bounded and free from any externally-imposed disturbances such as inward-running shock waves. Thus denoting $Me_N = Me \sin \phi$ we have the requirements

$$\tilde{H}(\delta) = 0 \quad (7)$$

$$\frac{d\tilde{P}}{dy}(\delta) = -i(\sqrt{Me_N^2 - 1})\tilde{P}(\delta) \quad (8)$$

which imply, respectively, that the perturbations become adiabatic and that the corresponding pressure field involves either simple Mach waves ($Me_N > 1$) or exponentially-decaying signals ($Me_N < 1$). Now consider the inner boundary conditions on the wall in the general case where there may be mass transfer across it, taking viscous and heat conduction effects into account. By overall mass conservation across the gas-solid interface, we have that

$$v(x, z, y_W) = \left(\frac{\dot{m}_{w0} + \Delta \dot{m}_w}{\rho_{g0}(x, z, y_W) + \rho_g} \right) - \frac{\dot{m}_{w0}}{\rho_{g0}(x, z, 0)}$$

where \dot{m}_{w0} is the mean surface mass loss rate, $\Delta\dot{m}_w$ its corresponding perturbation due to ablative response to boundary layer heat transfer perturbations (as calculated below), and ρ_g the density in the gas phase. In terms of the foregoing complex notation, this boundary condition becomes

$$\tilde{V}(0) = \frac{\Delta\dot{m}_w}{\rho_{g0}(0)} - \frac{\dot{m}_{w0}}{\rho_{g0}(0)} \left(\frac{i\varepsilon}{h_{0w}} \frac{dH_0}{dy}(0) + \tilde{\rho}(0) \right) \quad (9)$$

The presence of viscosity requires the no slip conditions which under the present approximations are that $W(x, z, y_w) = U(x, z, y_w) = 0$; hence we obtain the single equivalent condition

$$\tilde{Q}(0) = i\varepsilon \frac{dq_0}{dy}(0) = i\varepsilon \left(\frac{\tau_{N0}}{\mu_{w0}} \right) \quad (10)$$

Finally, there are the thermal boundary conditions on the surface. If it is non-ablating and held at some fixed temperature T_{w0} we require on the mean line that

$$T'(x, z, 0) = -y_w \left(\frac{dT_0}{dy} \right) \quad \text{or}$$

$$\tilde{H}(0) = i\varepsilon \frac{dH_0}{dy}(0) \quad (11a)$$

whereas if the surface heat transfer rate is considered fixed, we require

$$\mu_{0w} \frac{d\tilde{H}(0)}{dy} + \tilde{\mu}(0) \frac{dH_0(0)}{dy} = 0 \quad (11b)$$

However, if the surface is undergoing rapid equilibrium steady-state sublimative ablation at some "ablation temperature" $(T_w)_{abl}$, such that the mass fraction of the ablation specie in the gas adjacent to the wall is essentially unity (i.e., the partial pressure is approximately equal to the total gas pressure), then neglecting gas phase chemical reactions leads to the condition that

$$h(x, z, y_w) = h_0(x, z, y_w) + \left(\frac{dh_{abl}}{dp} \right)_0 (p_w - p_\infty) \quad \text{or}$$

$$\tilde{H}(0) = i\epsilon \frac{dH_0(0)}{dy} + \left(\frac{dh_{abl}}{dp} \right)_0 \tilde{P}(0) \quad (11c)$$

where the Clausius - Clapyron relationship $\frac{dh_{abl}}{dp} = \frac{R_{abl} T_{abl}^2}{p L_{vap}}$ gives the equilibrium ablation temperature as a function of pressure, the ablation material gas constant R_{abl} and the heat of vaporization L_{vap} . It is noted that the foregoing boundary conditions must be replaced by an alternative set of conditions when only the inviscid part of the perturbation solution is sought, as discussed below.

Once the perturbation equations are solved, the results can be used to calculate a number of important physical features of the flow. Thus, for example, the skin friction is

$$\tau = \left(\mu \frac{du}{dy} \right)_w \sin\phi - \left(\mu \frac{dw}{dy} \right)_w \cos\phi$$

which yields in the present approximation the perturbation

$$\tau - \tau_{N_0} = \text{Re}(\Delta\tilde{\tau} \exp i\alpha\xi) \quad \text{where}$$

$$\tau_{N_0} = \mu_{w_0} \frac{dq_0}{dy}(0) \quad \text{and}$$

$$\Delta\tilde{\tau} = \mu_{w_0} \frac{d\tilde{Q}}{dy}(0) + \tilde{\mu}(0) \frac{dq_0}{dy}(0) \quad (12)$$

Correspondingly, the net perturbation in the transfer to the surface from the gas (allowing in the general case for heat convection due to ablation) is

$$\Delta\dot{\tilde{q}}_w = \text{Re}(\Delta\dot{\tilde{q}}_w \exp i\alpha\xi) \quad \text{where}$$

$$\Delta\dot{\tilde{q}}_w = \mu_{0w} \frac{d\tilde{H}}{dy}(0) + \tilde{\mu}(0) \frac{dH_0}{dy}(0) - \dot{m}_{w_0} \tilde{H}(0) - h_{0w} \Delta\dot{\tilde{m}}_w \quad (13)$$

2.2 Inviscid solutions

Consider now the inviscid part of the disturbance field as determined by discarding the viscous terms on the right hand sides of eqs (2-4). Lighthill (ref. 7) has shown from these equations that the pressure field \tilde{P} can be described independently of the velocity, density and temperature by the following second order linear differential equation involving only the mean flow Mach number profile:

$$\left\{ \frac{d^2}{dy^2} - 2 \left(\frac{dM_0/dy}{M_0} \frac{d}{dy} + \alpha (M_{0N}^2 - 1) \right) \right\} \tilde{P} = 0 \quad (14)$$

Once this equation is solved, the corresponding inviscid velocity and enthalpy perturbations follow directly from eqs. (2-4). In particular eq. (4) yields the interesting result that

$$\tilde{H}(y)_{\text{inviscid}} = \left(\frac{dH_0/dy}{\alpha} \right) i \frac{\tilde{V}}{q_0} (y) \quad (15)$$

which shows that the total enthalpy perturbation in the inviscid flow is proportional to the local mean flow total enthalpy gradient and the local perturbed streamline slope and has a maximum exactly in the streamline valleys (i.e., \tilde{H} leads \tilde{V} by $\frac{\pi}{2}$) regardless of the edge Mach number.

The solution of eq. (11) must satisfy the outer boundary condition (8); the proper inner boundary condition to use, however, requires some care since the solution possesses a singularity at $y = 0$ where $M_0 \rightarrow 0$ (refs. 7,8). This difficulty can be avoided by imposing a kinematical tangency condition $v' = q_0(dy_w/dx) = \epsilon \alpha q_0(y_f) \cos \alpha \xi$ for a wavy wall placed at some appropriate level $y_f > 0$ (such that $q_0(y_f) > 0$) above the actual surface; thus, substituting $\tilde{V} = \epsilon \alpha q_0$ into the inviscid form of eq. (3), one finds the equivalent inner inviscid boundary condition:

$$\frac{d\tilde{P}}{dy} (y_f)_{\text{inviscid}} = - i \epsilon \alpha^2 (\rho_0 q_0^2)_{y_f} \quad (16)$$

On physical grounds, this "out-off" distance y_f represents the viscous displacement effect due to the influence of viscosity (no slip) on the perturbation velocity field near the surface; it can be specified by a consideration of these viscous effects, as described below.

Various methods of solution to eq. (14) have been studied by previous investigators. Lighthill (ref. 7) examined the general analytical structure of its two linearly-independent solutions, and also discussed closed form asymptotic solutions in the limits of either small or large $\alpha\delta$ values. Application to a highly-idealized wavy wall problem, wherein the boundary layer is approximated by a Mach number discontinuity so as to obtain a closed form solution, has been studied by Inger (ref. 13). The results indicated that the mean boundary layer vorticity can significantly influence the wall pressure signature and hence that a more detailed numerical study of solutions to eq. (14) for realistic boundary layer profiles was warranted. Some preliminary results of such a study have been obtained for a continuous Mach number distribution representative of a turbulent boundary layer (ref. 14). An important feature of the study was the development of a novel "top down" integration scheme whereby the split boundary value problem for eq. (14) is converted into an equivalent but more tractable initial value problem. In this scheme, a downward integration is initiated at $y = \delta$ with the known solution for uniform flow past a wavy wall; then, at any $0 < y < \delta$ within the boundary layer, the resulting $\tilde{P}(y)$ defines a streamline via eq. (3) to which an effective wavy wall of different amplitude and phase (relative to those at the outer edge) can be matched. By simply correcting for these known amplitude and phase distortions, the true pressure signature on a wavy wall of amplitude ϵ placed at the desired level can be determined. The inward march of this top down calculation is truncated at the effective wall position $y = y_f$.

Numerical solutions of eq. (14) by the aforementioned "topdown" integration method have been obtained for turbulent boundary layer Mach number profiles appropriate to available wavy wall experiments (ref. 6). An accurate analytical representation of these profiles for this purpose was obtained based on the theoretical model of Sontowski (ref. 15) as described in ref. 6. Figure 2 shows some typical variations of the pressure amplitude (relative to uniform potential flow) across the boundary layer, including details of the behavior approaching the cut-off near the surface. It is seen that the non-uniform velocity field of the boundary layer causes a large decrease of this relative amplitude at transonic edge Mach numbers. It is also interesting to note that, in agreement with the predictions of Inger's simplified model solution (ref. 13), there is evidently some special Mach number in the vicinity of $M_e \sim \sqrt{2}$ where virtually no amplitude change occurs across the layer. Figure 3 illustrates the corresponding phase variations of the pressure across the boundary layer. A significant shift of the pressure maximum toward the wavy wall valley is seen to occur as a result of the wave reflections from the boundary layer profile when $M_e < 2$. Clearly, the nonuniform flow can cause a predominantly subsonic pressure signature to exist on a wavy wall when the external inviscid flow is weakly -to- moderately supersonic.

2.3 Viscous and heat conduction effects in the boundary layer

We now consider the solution of the full eqs. (1-5). Numerical solutions of this formidable set of equations have been studied by Brown (ref. 12) and Lew and Li (ref. 16); however, in the present work, we shall seek to illuminate the essential physics of the viscous sublayer behavior by means of approximate analytical solutions. To this end, we introduce the following simplifying assumptions:

(a) Viscous dissipation heating effects on both the mean and perturbed flows are neglected, which is consistent with the already-accepted limitation to moderate supersonic Mach numbers;

- (b) Viscosity and heat conduction effects on the perturbation field lie essentially within a thin "frictional sublayer" whose thickness δ_f is small compared to the boundary layer thickness;
- (c) In the case of turbulent motion, this friction sublayer lies within the so-called laminar sublayer such that the mean velocity and temperature profiles are approximately linear;
- (d) The frictional sublayer is also small compared to the disturbance wavelength such that $(\alpha \delta_f)^2 \ll 1$, which is quite accurate for conditions of practical interest;
- (e) Although compressibility effects due to heat transfer on the mean flow are taken into account by an appropriate coordinate transformation, the density and viscosity perturbations are still neglected, an approximation validated by the work of Lew and Li (ref. 16);
- (f) We take $\rho_0 \mu_0 = \text{constant}$.

Introducing the compressibility transformations

$$Y = \int_0^y \left(\frac{\rho_0}{\rho_{0w}} \right) dy \quad (17)$$

$$\tilde{V}^* = \frac{\rho_0 \tilde{V}}{\rho_{0w}} \quad (18)$$

and the aforementioned assumptions into eqs. (1-5), they greatly simplify to the following :

$$i\alpha \tilde{Q} + \frac{d\tilde{V}^*}{dY} = 0 \quad (19)$$

$$i\alpha q_0 \tilde{Q} + \left(\frac{dq_0}{dY} \right) \tilde{V}^* + \left(\frac{H_0}{h_{0w}} \right) \frac{i\alpha \tilde{P}}{\rho_{0w}} = v_{0w} \frac{d^2 \tilde{Q}}{dY^2} \quad (20)$$

$$i\alpha q_0 \tilde{H} + \left(\frac{dH_0}{dY} \right) \tilde{V}^* = v_{0w} \frac{d^2 \tilde{H}}{dY^2} \quad (21)$$

with $\frac{d\tilde{P}}{dY} = 0$, (i.e., \tilde{P} is constant across the friction layer

as determined by the inviscid solution described above) and where

$$q_0 = \left(\frac{dq_0}{dY} \right)_w Y \approx \frac{\tau_{N_0} Y}{\mu_{w_0}}$$

$$\frac{H_0}{h_{0w}} \approx 1 + \left(\left(\frac{dH_0}{dY} \right)_w / h_{0w} \right) Y$$

and ν_{w_0} is the kinematic viscosity. Note that the energy equation (21) has been uncoupled from the others. The outer boundary conditions to impose are that the viscous parts of the solutions for \tilde{Q} , \tilde{V} , and \tilde{H} decay exponentially as $y \gg \delta_f$, whereas the inner boundary conditions are given by eqs (9-11) with $\tilde{u} = \tilde{p} = 0$ and \tilde{V}^* , Y replacing \tilde{V} , y respectively.

In connection with the foregoing equations, it is noted that all terms explicitly involving the mean surface mass flow that would otherwise appear have been neglected even though we do in fact allow such a mass flow to be present. Not only is such an approximation consistent with our basic parallel mean flow model but it is also known to be a reasonable engineering approximation in estimating ablation material response to boundary layer disturbances (ref. 17).

The solution for the velocity perturbation field is obtained as follows. Combining eqs.(19) and (20) by differentiation so as to eliminate \tilde{Q} , we obtain a non-homogeneous Orr-Sommerfeld equation for \tilde{V} alone:

$$\left\{ \nu_{w_0} \frac{d^2}{dY^2} - i\alpha \frac{\tau_{N_0}}{\mu_{w_0}} Y \right\} \frac{d^2 \tilde{V}^*}{dY^2} \approx \frac{\alpha^2}{\rho_{0w}} \left[\frac{dH_0/dY(0)}{h_{0w}} \right] \tilde{P}(0) \quad (22)$$

where the new non-homogeneous term on the right side represents the influence of the mean flow heat transfer on the perturbation pressure gradient. It is immediately seen that the characteristic thickness of the frictional sublayer must be

$$\delta_f = (\mu_0^2 / \rho_0 \tau_{N_0} \alpha)^{1/3}.$$

Now by introducing $\zeta = y/\delta_f$, the homogeneous part of eq. (22) assumes the form of an Airy equation in $d^2\tilde{V}/d\zeta^2$, whose solution is of the form

$$\tilde{V} = A + B\zeta + c\chi(\zeta)$$

where

$$\chi(\zeta) \equiv \int_{\infty}^{\zeta} \left[\int_{\infty}^{\zeta} \zeta^{1/2} H_{1/3}^{(1)} \left(\frac{2}{3} (i\zeta)^{3/2} \right) d\zeta \right] d\zeta \quad (23)$$

is an exponentially-decaying function having the properties

$$\chi(\infty) \rightarrow 0 \quad \text{and} \quad \chi(0) = 2\pi/3$$

$$\frac{\chi'(0)}{\chi(0)} = -1.29 \exp\left(\frac{\pi i}{6}\right)$$

$$\frac{\chi''(0)}{\chi'(0)} = -1.067 \exp\left(\frac{\pi i}{6}\right)$$

$$\frac{\chi'''(0)}{\chi''(0)} = -7.29 i \exp\left(-\frac{\pi i}{3}\right).$$

The corresponding particular non-homogeneous solution of eq. (22) can be constructed by analogy with the analysis given by Holstein (ref. 18) such that the complete solution can be written as

$$\tilde{V}^*(\zeta) = A + B\zeta + c\chi(\zeta) + \frac{i\alpha l}{\rho_{0w}} \left(\frac{dH_0/dY}{dq_0/dY} \right)_w \tilde{P}(0) \cdot I(\zeta) \quad (24)$$

where $I = \int_0^{\zeta} \int_0^{\xi} G d\xi d\zeta$ and G is a function defined and tabulated by Holstein with the properties that $G(\zeta) = \zeta^{-1}$ as $\zeta \gg 1$, $G(0) = 1.285 i$ and $G'(0) = .937$. Application of the inner boundary conditions (9) and (10), using eq. (19) serves to determine the constants A and B and thereby to re-express \tilde{V}^* in terms of the single constant $C = -c\chi'(0)$. Then, requiring

that the resulting solution for \tilde{Q} from eqs. (19) and (24) match at $\zeta \gg 1$ with the inviscid solution given by the left hand side of eq. 2 evaluated near the surface, and making use of the asymptotic property that $I + \zeta(1 - \frac{dI}{d\zeta}) \rightarrow .939i$ for $\zeta \gg 1$, one finds the value of C to be

$$C = 1.29 \, i \epsilon \alpha \delta_f \left(\frac{\tau_{N_0}}{\mu_{w_0}} \right) \Omega_p \, e^{\pi i/6} \left(1 + .939i \left(\frac{\delta_f}{h_{0w}} \right) \frac{dH_0}{dY}(0) \right) \quad (25)$$

where $\Omega_p = \alpha \delta_f^2 \tilde{P}(0) / \epsilon \tau_{N_0}$ is the ratio of pressure to viscous forces in the perturbation field. Hence the \tilde{V}^* solution assumes the final form

$$\begin{aligned} \tilde{V}^* - \tilde{V}^*(0) = & \epsilon \alpha q_0(Y) + 1.29 \epsilon \alpha \delta_f \left(\frac{\tau_{N_0}}{\mu_{w_0}} \right) \Omega_p e^{7\pi i/6} \times \\ & \times \left[\left(\zeta - \frac{\chi(\zeta)}{\chi'(0)} - .776 e^{-\frac{\pi i}{6}} \right) \left(1 + .939i \left(\frac{\delta_f}{h_{0w}} \right) \frac{dH_0}{dY}(0) \right) + \right. \\ & \left. + .776 e^{-\frac{\pi i}{6}} I(\zeta) \left(\frac{\delta_f}{h_{0w}} \right) \frac{dH_0}{dY}(0) \right] \quad (26) \end{aligned}$$

The first term on the right is the inviscid part of the solution which satisfies the kinematic tangency condition on a wavy wall placed a distance Y above the mean surface. The second term represents the viscous displacement effect discussed by Lighthill (ref. 8), here generalized to include the effect of compressibility due to heat transfer in the mean flow. Following Lighthill and viewing this second term from a large distance from the wall when $\zeta \gg 1$ ($\chi \rightarrow 0$; $I \rightarrow \zeta \ln \zeta$), it effectively vanishes at

$$\zeta_f = .776 e^{-\frac{\pi i}{6}} \left[1 + \frac{.776 e^{-\frac{\pi i}{6}} \left(\frac{\delta_f}{h_{0w}} \right) \frac{dH_0}{dY}(0)}{1 + .939i \left(\frac{\delta_f}{h_{0w}} \right) \frac{dH_0}{dY}(0)} \right] \ln \zeta \quad (27)$$

which thereby defines an effective friction sublayer thickness or equivalent wall position in a purely inviscid solution which is proportional to $(\mu_{w0}^2 / \rho_{0w} \tau_{N0} \alpha)^{1/3}$. Thus, eq. (27) provides the effective cut-off distance for the inviscid solution discussed earlier.

The complex shear stress perturbation in the present approximation is found to be

$$\begin{aligned} \Delta \tilde{\tau} &= \mu_{0w} \frac{d\tilde{Q}}{dY} (0) = \frac{i\mu_{0w}}{\alpha} \frac{d^2 \tilde{V}^*}{dY^2} (0) \\ &= 1.37 \tau_{N0} \frac{\epsilon \Omega p}{\delta_f} e^{\frac{4}{3} i\pi} \left(1 + 1.62 e^{\frac{\pi i}{3}} \left(\frac{\delta_f}{h_{0w}} \right) \frac{dH_0}{dY} (0) \right) \quad (28) \end{aligned}$$

whose amplitude is proportional to the mean shear stress and the inverse of the friction sublayer thickness with a phase which lags the pressure by an angle ranging from 120° in the case of a very weak mean heat transfer rate to 60° in the opposite limit of large heat transfer. This result forcefully illustrates the error associated with the frequently-made a priori assumption that $\tau' \sim p'$.

Turn now to a consideration of the energy transfer within the friction sublayer, a feature of the sinusoidal perturbation problem heretofore ignored in the literature. To this end, it is convenient to recast eq. (21) in terms of the new Crocco-like enthalpy variable $\tilde{H}^* \equiv \tilde{H} - C_0 \tilde{Q}$ where $C_0 = (dH_0/dy)_w / (dq_0/dy)_w$ is a kind of Reynolds analogy factor and the mean flow obeys the Crocco relation $H_0(Y) = h_{0w} + C_0 q_0(Y)$. Then multiplying eq. (20) by C_0 and subtracting the result from eq. (21) yields

$$\left\{ \nu_{0w} \frac{d^2}{dY^2} - i\alpha \left(\frac{\tau_{N0}}{\mu_{w0}} \right) Y \right\} \tilde{H}^* = - \frac{i\alpha C_0 \tilde{P}}{\rho_{0w} h_{0w}} \left(h_{0w} + C_0 \left(\frac{\tau_{N0}}{\mu_{w0}} \right) Y \right) \quad (29)$$

from which V^{**} has now been eliminated. Appropriate to eq. (29) we have the following wall boundary condition options in terms of the variable H^{**} :

$$H^{**}(0) = 0 \quad (\text{fixed wall temperature}) \quad (30A)$$

$$\frac{dH^{**}}{dY}(0) = -C_0 \frac{d\tilde{q}}{dY}(0) \quad (\text{fixed heat transfer}) \quad (30B)$$

$$H^{**}(0) = \left(\frac{RC_p T_w^2}{L_{vap}} \right)_{abl.} \frac{\tilde{P}(0)}{P_\infty} \quad (\text{rapidly ablating wall}) \quad (30C)$$

The appropriate boundary condition on \tilde{H}^{**} at large ζ (as inferred from eq. 13) is that

$$\tilde{H}^{**} = \tilde{H}^{**}_{inviscid} = \frac{C_0 \tilde{P}}{\tau_{0N} \gamma / \nu_{0W}} = \frac{\alpha \delta_f^2 C_0 \tilde{P}}{\mu_{0W}} \quad (31)$$

Now a comparison of eqs. (22) and (29) shows that the complementary homogeneous solution of the latter is proportional to \tilde{V}'' , and hence χ'' , which decays exponentially for $\zeta \gg 1$. Furthermore, taking $\tilde{P} = \text{constant}$ across the friction sublayer, a particular non-homogeneous integral of eq. (29) which satisfies the outer condition (31) can be readily found to be proportional to the functional combination:

$$G + \frac{C_0 \delta_f}{h_{0W}} \left(\frac{\tau_{0N}}{\mu_{0W}} \right).$$

Hence, the complete solution can be written as

$$\tilde{H}^{**} = D \chi''(\zeta) + \frac{\alpha \delta_f^2 C_0 \tilde{P}}{\mu_{0W}} \left(G(\zeta) + \frac{C_0 \tau_{0N} \delta_f}{\mu_{0W} h_{0W}} \right) \quad (32)$$

where D is a constant determined by the aforementioned boundary conditions (30). Hence, in the case of a fixed wall temperature, we find that the complex heat transfer perturbation to the

surface is

$$\tilde{\Delta \dot{q}}_w \approx .433 \mu_{w0} \frac{dH_0}{dY} (0) \frac{\epsilon}{\delta_f} \Omega_p e^{3\pi i} \left(1 + 5.40 \left(\frac{\delta_f}{h_{w0}} \right) \frac{dH_0}{dY} e^{\frac{13\pi i}{30}} \right) \quad (33)$$

where the second term in brackets represents the compressibility effect of the mean flow heat transfer. Since the right side is proportional to the mean heat transfer rate, eq. (33) shows that when the mean boundary layer flow is adiabatic, so will be the motion in the frictional sublayer. Furthermore, this equation shows that the heat transfer perturbation lags the pressure (Ω_p) by an angle ranging from 120° in the weak mean heat transfer case to about 42° in the case of strong heat transfer. Hence, the frequently used a priori assumption that $\Delta \dot{q}_w \sim p'$ can be appreciably in error.

Turning to the case of a prescribed heating rate to the wall, eqs. (30B) and (32) yield the surface temperature perturbation as

$$\begin{aligned} c_p \tilde{T}(y_w) &= \tilde{H}(0) - i\epsilon \frac{dH_0}{dY} (0) \\ &= .595\epsilon \frac{dH_0}{dY} (0) \Omega_p e^{\frac{7\pi i}{6}} \left(1 + 5.40 \left(\frac{\delta_f}{h_{0w}} \right) \frac{dH_0}{dY} (0) e^{\frac{.433\pi i}{30}} \right) \end{aligned} \quad (33)$$

Thus for a small fixed rate of heat loss from the surface ($dH_0/dY < 0$), as was the case in the wavy wall experiments of ref. 6 described below, eq. (33) predicts in the leading approximation that the wall temperature perturbation leads the pressure by only 30° , i.e., that T'_{\max} and p'_{\max} are strongly correlated. This is corroborated by temperature-sensitive liquid crystal paint observations (ref. 6).

Finally, in the ablating wall case, eqs. (30C) and (32) yield the following gas phase relations that will be useful later :

$$\tilde{H}(0) = i\epsilon \frac{dH_0}{dY}(0) + \left(\frac{R C_p T_w^2}{L_{vap}} \right)_{abl.} \frac{\tilde{P}(0)}{p_\infty} \quad (34)$$

$$\frac{d\tilde{H}}{dY}(0) = .729 \frac{e}{\delta_f} \frac{7\pi i}{6} \left(\tilde{H}(0) - i\epsilon \frac{dH_0}{dY} \right) + \left(\frac{\Delta \tilde{q}_w}{\mu_{w0}} \right)_{eq.33} \quad (35)$$

Figure 4 gives a schematic summary of the main qualitative results of the present analysis on the relative phasing of the surface pressure, shear and heat transfer perturbations for the case of fixed surface temperature. In general, there are two different physical extremes: the first pertains to either subsonic external flow or supersonic external flow with a relatively thick boundary layer $\alpha\delta_0 > 1$ such that the flow near the wall is effectively subsonic; the second pertains to supersonic external flow with $\alpha\delta_0 \ll 1$ such that the pressure field is effectively an inviscid supersonic one. In the former regime, the maximum pressure occurs in the surface valleys while the shear and heat transfer maxima lie either slightly downstream of the maximum slope points in the case of weak mean heat transfer (in agreement with Benjamin's analysis (ref. 9)) or between the valleys and the maximum slope points in the opposite case of large heat transfer. Clearly, when the heat transfer rate and $\alpha\delta_0$ are both sufficiently large, the heat transfer perturbation can have a significant component in the valleys of the surface. In the other regime where $\alpha\delta_0 \ll 1$, all these maxima have shifted downstream so as to place the pressure maximum at its 'linearized' supersonic position and the shear and heat transfer maxima around the surface crests. In all cases, it is noted that the shear and heat transfer perturbations are nearly in phase.

3. DISTURBANCES WITHIN A RAPIDLY
ABLATING WAVY WALL

3.1 General considerations

The foregoing analysis presents a set of approximate relations governing the gas dynamic disturbances within the boundary layer adjacent to a wavy wall, including the possibility of mass loss from the surface. In this section, we now seek to examine the corresponding ablative response of the wall material to these boundary layer disturbances and the resulting interaction (and possible resonance) of the two.

The interaction between the boundary layer and the ablating material is described by an energy flux conservation relation across the gas-solid interface on the wavy wall surface, which reads

$$\left(\mu \frac{dH}{dy}\right)_{g,w} - \dot{m}_{wg} h_{g,w} = \lambda_s \left(\frac{dT}{dy}\right)_w - \dot{m}_{ws} h_{s,w} \quad (36)$$

where λ_s is the thermal conductivity of the wall material, assumed constant, T_s its temperature and $\dot{m}_{wg} = \dot{m}_{ws} = \dot{m}_w$ by interfacial mass conservation. Accompanying eq. (36) is the requirement that the temperature be continuous across the interface, i.e., that $T_{gw} = H_w/C_{pg} = T_{sw}$. Now application of eq. (36) to the mean surface yields

$$\mu_0 \frac{dH_0}{dy}(0) - \dot{m}_{w0} (h_{g0}(0) - h_{s0}(0)) = \lambda_s \frac{dT_{s0}}{dy}(0) \quad (37)$$

where $h_{g0} - h_{s0} = (C_{pg} - C_{ps})T_{wabl} + L_{vap}$ is the effective energy absorbed by the mean ablation rate. Furthermore, when applied to the first order perturbation effects on both sides of the interface, after subtracting out eq. (37) and transferring to the mean surface, eq. (36) yields in the present approximation that

$$\begin{aligned} \mu_{w_0} \frac{d\tilde{H}}{dY}(0) - \dot{m}_{w_0} (\tilde{H}(0) - i\epsilon \frac{dH_0}{dY}(0) - C_{p_s} \tilde{T}_s(0)) - (h_{g_0}(0) - h_{s_0}(0)) \Delta \dot{m}_w \\ \approx \lambda_s \frac{d\tilde{T}_s}{dy}(0) \end{aligned} \quad (38)$$

where $T'_s = T_s - T_{s_0} = \text{Re}(\tilde{T}_s \exp i\alpha\xi)$ is the material temperature distribution perturbation and where use has been made of the approximation $d^2H_0/dY^2(0) \approx 0$ and the fact (see below) that $\lambda_s (d^2T_{s_0}/dy^2)_w = \dot{m}_{w_0} C_{p_s} (dT_{s_0}/dy)_w$. Once the heat conduction equation for the ablating solid is solved for the mean and perturbed material temperature fields, the corresponding ablative mass losses from the surface can be determined from eqs. (37) and (38).

3.2 Perturbation analysis of the heat conduction equation

Within the solid material presumed to underly the stationary rippled surface illustrated in fig. 1, the temperature distribution $T_s(x, y, z)$ in the presence of a quasi-steady ablative mass loss at the surface is given by the three dimensional heat conduction equations

$$\lambda_s \left[\frac{d^2}{dx^2} + \frac{d^2}{dy^2} + \frac{d^2}{dz^2} \right] T_s \approx \dot{m}_w \frac{dT_s}{dy} \quad (39)$$

where we assume that deep within the material ($y \rightarrow -\infty$) T_s approaches some fixed interior value T_{s_i} . Guided by considerations similar to those used in treating the boundary layer gas phase perturbations, we write $T_s = T_{s_0}(y) + \text{Re}(\tilde{T}_s(y) \exp i\alpha\xi)$ and by substituting into eq. (39) find that the mean and perturbation temperature fields, respectively, are governed by the relations

$$\lambda_s \frac{d^2T_{s_0}}{dy^2} = C_{p_s} \dot{m}_{w_0} \frac{dT_{s_0}}{dy} \quad (40)$$

$$\lambda_s \left(\frac{d^2\tilde{T}_s}{dy^2} - \alpha^2\tilde{T}_s \right) - C_{p_s} \dot{m}_{w_0} \frac{d\tilde{T}_s}{dy} \approx \left(C_{p_s} \frac{dT_{s_0}}{dy} \right) \Delta \dot{m}_w \quad (41)$$

where it is noted that the term $\alpha^2 \tilde{T}_s$ on the left side of eq. (41) represents the effect of heat conduction in the ξ -direction, while the non-homogeneous term on the right side is due to the convective heat loss associated with the surface ablation rate perturbation. The solution of eq. (40) subject to the boundary conditions $T_{s_0}(0) = T_{w_{abl}}$ and $T_{s_0}(-\infty) = T_{s_i}$ is the well-known exponential

$$\frac{T_{s_0}(y) - T_{s_i}}{T_{s_0}(0) - T_{s_i}} = \exp\left(\frac{\dot{m}_{w_0} y}{\lambda_s / C_{ps}}\right) \quad (42A)$$

with

$$\lambda_s \frac{dT_{s_0}}{dy}(0) = \dot{m}_{w_0} C_{ps} (T_{w_{abl}} - T_{s_i}) \quad (42B)$$

The corresponding solution of eq. (41) which vanishes exponentially far below the surface is readily found and yields the following expression for the complex conductive heat transfer perturbation at the surface:

$$\lambda_s \frac{d\tilde{T}_s}{dy}(0) = (1 + \sqrt{1+k^2}) \frac{C_{ps} T_s(0)}{2} \dot{m}_{w_0} + 2 \left(\frac{\sqrt{1+k^2}-1}{k^2} \right) C_{ps} (T_{abl} - T_{s_i}) \Delta \dot{m}_{w_0} \quad (43)$$

where $\tilde{T}_s(0) = i\epsilon(dT_{s_0}/dy)_w + (\tilde{H}(0) - i\epsilon(dH_0/dy)_w) / C_{pg}$ by virtue of temperature continuity across the interface and where the parameter $k \equiv 2\lambda_s \alpha / C_{ps} \dot{m}_{w_0} \sim$ (streamwise heat conduction/ablative heat loss) is introduced directly by the second term on the left of eq. 41. As inspection of eq. 43 shows, this parameter is an important one in controlling the contribution of the ablation rate perturbation to the interfacial heat balance.

3.3 Ablation rate perturbation

Combining eqs. (37) and (42B) serves to determine the mean surface mass loss rate in terms of known quantities as

$$\dot{m}_{w0} \approx \frac{\mu_{w0} (dH_0/dy)_w}{h_{g0}(0) - h_{si}} \approx \frac{\mu_{w0} \frac{dH_0}{dy}(0)}{L_{vap} + C_{pg} T_{abl}} \quad (44)$$

since $T_{abl} \gg T_{si}$. Thus from (42B) the mean heat conduction into the solid is but a small fraction of the boundary layer heat transfer to the surface :

$$\frac{\lambda_s (dT_{s0}/dy)_w}{\mu_{w0} (dH_0/dy)_w} \approx \left(\frac{h_{s0} - h_{si}}{h_{g0} - h_{si}} \right) \approx \frac{C_{ps} T_{abl}}{L_{vap} + C_{pg} T_{abl}} \quad (45)$$

Turning to the perturbation problem, eq. (38) and (43) yield the following expression governing $\Delta \dot{m}_w$ upon using eqs. (33)-(35) and (45) :

$$\begin{aligned} \frac{\Delta \dot{m}_w}{\dot{m}_{w0} / \delta_f} (1 + a_k) &\approx .433 \Omega_p e^{\frac{4}{3} \pi i} (1 + 5.40 e^{\frac{13\pi i}{30}}) \left(\frac{\delta_f}{h_{gw}} \right) \left(\frac{dH_0}{dY} \right)_w \\ &- \frac{c_{ps} \mu_{w0}}{2\lambda_s} \frac{h_{s0}(0)}{h_{g0}(0)} (\sqrt{1+k^2} - 1) e^{\frac{\pi i}{2}} \left(\frac{\delta_f}{h_{gw}} \right) \left(\frac{dH_0}{dY} \right)_w \\ &- B \left[.729 e^{\frac{\pi i}{6}} + \left(\frac{\delta_f}{h_{gw}} \right) \left(\frac{dH_0}{dY} \right) \right] \end{aligned} \quad (46A)$$

where $a_k \equiv (h_{s0}/h_{g0}) \left[(2(\sqrt{1+k^2}-1)/k^2) - 1 \right]$ and the parameter

$$B = \left(\frac{R \Omega_p T_w^2}{L_{vap}} \right)_{abl} \frac{\tilde{P}(0)/p_\infty}{\epsilon (dH_0/dy)_w} \quad (46B)$$

represents the ratio of the ablation material enthalpy change from a pressure disturbance to the ablative energy absorption

caused by the boundary layer heat transfer perturbation. Since $h_{s_0} \ll h_{g_0}$, a_k is always small compared to unity for all values of k and hence is not a significant parameter. Similarly, under the conditions of strong ablation and heat transfer to which the present approximations pertain, the parameter B is small compared to unity and can therefore be dropped from eq. (46A) with little error.

In the limit of strong heat transfer, eq. (46A) can thus be simplified to the following leading approximation:

$$\frac{\dot{\Delta m}_w}{\dot{m}_{w_0}} \approx \frac{\epsilon \frac{dH_0}{dY}(0)}{h_{g_0}(0)} \left[2.34 \Omega_p e^{-\frac{7\pi i}{30}} - \frac{c_{ps} \mu_{w_0} h_{s_0}(0)}{2\lambda_s h_{g_0}(0)} (\sqrt{1+k^2}-1) e^{\frac{\pi i}{2}} \right] \quad (47)$$

Without resorting to a detailed parametric study of this equation, a qualitative analysis can be made which demonstrates the existence of a resonant interaction between the boundary layer and ablation perturbations at one particular wavelength or "eigenvalue" $\alpha\delta_0$. Consider the component of mass loss perturbation in the surface valleys (i.e., the imaginary part of (47)) which in terms of $\Omega_p = |\Omega_p| e^{i\phi_p}$ is proportional to

$$2.34 |\Omega_p| \sin(\phi_p - 42^\circ) - \frac{c_{ps} \mu_{w_0} h_{s_0}(0)}{2\lambda_s h_{g_0}(0)} (\sqrt{1+k^2}-1) \quad (48)$$

Now in the thin boundary layer limit $\alpha\delta_0 \ll 1$ where $\phi_p \rightarrow 0$ and $k \sim \alpha\delta \rightarrow 0$, eq. (48) shows that the valley mass loss perturbation is negative. However, in the opposite limit $\alpha\delta_0 \gg 1$ where $\phi_p \rightarrow \frac{\pi}{2}$, a positive value can appear depending on the magnitude of the streamwise heat conduction parameter k . Since k itself is proportional to α and numerical results indicate that (ref. 6, 14) $\Omega_p \rightarrow \text{constant}$ when $\alpha\delta_0 \gtrsim O(1)$, it is seen that a maximum positive value of eq. (48) must occur at one particular value of $\alpha\delta_0$ (on the order of unity). This is illustrated by the sketch in fig. 5 which shows the qualitative behavior of eq. 48 as a function of $\alpha\delta_0$ with $\frac{k}{\alpha}$ as a parameter. Provided the streamwise heat conduction within the ablation material is taken into

account, the present theory indicates that there is a critical wavelength of the surface waves (depending on the combined gas dynamic and wall material properties) at which the ablation rate in the valleys is a maximum and hence at which a self-perpetuating resonant interaction between the boundary layer and ablation surface perturbations can occur. Such a result is of obvious importance in possibly explaining the occurrence of ablation surface cross hatching patterns (ref. 5) and also in suggesting how they may be eliminated by altering the surface material to change the magnitude of the significant parameter k .

4. COMPARISONS WITH EXPERIMENT

Recently, a set of experiments were carried out (ref.6) on 2-dimensional compressible turbulent boundary layer flow past a wavy wall. Since these experiments afford an opportunity to evaluate a number of important aspects of the present theoretical analysis, a short account of them and comparisons of the results with theory will be presented here.

4.1 Brief description of tests

The purpose of the experiment was to measure the pressure and temperature along a simulated doubly-infinite sinusoidal surface in the presence of a fully-developed turbulent boundary layer at transonic and low supersonic speeds. It was carried out in a standard industrial-type "Trisonic" wind tunnel, a standard blowdown-to-atmosphere facility with a one foot square test section in which the Mach number is continuously variable from .3 to 1.25 and is obtainable from 1.4 to 3.5 by the use of fixed nozzle blocks. An aluminum wavy wall model replaced the entire vertical side wall and was centered about the transonic viewing window in the opposite side. The model incorporated a three cycle, two-dimensional sine wave which spanned the test section from top to bottom normal to the wind tunnel free stream flow. The wave pattern had a one inch wavelength with an amplitude of .030 inch. The transonic test section was used at all times, the remaining three walls being porous for the transonic runs but replaced with solid surfaces for the supersonic runs. Overall tests were conducted in a Mach number range from 0.8 to 1.8 with unit Reynolds numbers from .5 to 1.5 millions per inch.

The wavy wall region was instrumented with thirty 0.030 inch diameter pressure taps distributed so as to measure the phase shift of the peak pressure and to determine if the phasing is identical along two adjacent waves. Five scanivalves with five psi pressure transducers accurate to one percent were

used to measure these pressures. In addition, the temperature distribution along the surface was measured by means of a liquid crystal paint strip on a 4" wide by 12" long acrylic insert on one side of the wavy wall model parallel to the pressure taps. This paint has the advantage of reversibility, fast response and the ability to map finer details which cannot be derived from thermocouples even at far greater expense (ref. 19). The temperature distributions were recorded with 35 mm camera placed normal to the plane of the model. It is noted that the typical free stream total temperatures in these tests were higher than the corresponding wall recovery temperatures; consequently, the wall was being cooled rather than being heated as in flight.

In addition to these measurements and prior to the wavy wall tests, surveys of the undisturbed boundary layer profile for each test condition were made using a standard twenty-tube survey rake. These surveys showed that the boundary layer was in a fully developed turbulent state in all cases. Some typical experimental Mach number profiles are shown here in fig. 6 while values of the measured boundary layer thickness are shown in fig. 7. Further details on the experimental arrangements and techniques can be found in ref. 6.

4.2 Pressure distribution results

One of the principal objectives of the wavy wall tests was to check the theoretically-predicted phase shift in pressure across the boundary layer due to the non-uniform flow (simple uniform supersonic inviscid flow theory places the maximum pressure at the maximum wall slope point). A comparison of the theoretical and experimental phase shifts over the complete range of test conditions is given in fig. 8. Qualitatively, the agreement is quite good as to trends with respect to both Mach and Reynolds number; quantitatively, the theory tends to overestimate the phase shift angle by about 20° in the transonic regime $M_e \leq 1.4$. A comparison of the corresponding results for

pressure amplitude is presented in fig. 9. It is seen that the magnitude of the pressure perturbation in the transonic regime is overestimated by the theory by a factor of two, although the main qualitative trends are again in good agreement with experiment. This is to be expected in view of the linearized nature of the theory (although it is to be noted that its inclusion of a nonuniform mean flow eliminates the $M = 1$ singularity otherwise associated with the linearized solution in uniform flow). Indeed, McClure (ref. 20) has found that non-linear effects were large enough even for only a three percent amplitude ratio $\frac{E}{\rho}$ to reduce the peak pressures by as much as a factor of two. His results also agree with ours in showing a decrease of this discrepancy with increasing Mach number.

An interesting feature of these experiments is the occurrence of a pronounced non-sinusoidal variation or cusping at transonic speeds. Near Mach one, the absolute value of the negative pressure coefficient becomes double that of the positive pressure. This can be seen in fig. 10 where the effect of Mach number on this cusping trend is clearly illustrated. Since the spacing of static pressure orifices was chosen to define the phase shift of the peak positive pressure, the details of these unexpectedly-cusped shapes are not too well defined. Some suggestion of this phenomenon is given by Hosokawa's treatment of transonic flow past a wavy wall (ref. 21).

4.3 Surface temperature results

As discussed above, the wall temperature variation along the wavy wall portion of the model shown on the figure was estimated directly from the color photograph and the liquid crystal color code. In all cases, an unmistakable oscillatory temperature variation in the streamwise direction was observed which was well correlated with the pressure disturbances. A typical example is shown in fig. 11, where the corresponding wall temperature and pressure coefficient variations of a given run are compared. Note that the pressure and temperature varia-

tions very nearly coincide, in qualitative agreement with the predictions of the theoretical analysis of Section 2. Although it is usually assumed without proof that heat transfer and insulated wall temperature disturbances are in phase with the corresponding pressure perturbations, it is believed that is the first time it has been theoretically proven and experimentally confirmed.

5. CONCLUDING REMARKS

The significant results of this investigation can be summarized as follows.

1. As a consequence of the parallel mean flow and small disturbance approximations, it was shown that a neglect of hypersonic viscous dissipation heating effects permits the swept wavy wall problem to be treated in terms of an equivalent two-dimensional flow perpendicular to the wave crests.
2. Theory and experiment agree in showing that large changes in phase and amplitude of the pressure and temperature perturbations can occur across a turbulent boundary layer along a wavy wall when the wavelength and boundary layer thickness are of the same order. Consequently, a subsonic wall pressure distribution can exist even when the local inviscid flow is moderately supersonic.
3. The present generalization of Lighthill's earlier work on viscous sublayer effects to include heat transfer and compressibility effects has shown that the heat transfer perturbations on a solid wall of fixed surface temperature can be significantly out of phase (60° to 120°) with the corresponding pressure perturbations, in contrast to what is often assumed a priori. In the case of a wall with a given small heat transfer loss from the surface, the theory predicts a close correlation between p' and T' and this has been confirmed by experiment.
4. In the case of a rapidly ablating wavy wall of a sublimative material, an approximate analysis shows that a resonant interaction between the gas dynamic and ablative material disturbances can occur at one particular wavelength provided streamwise heat conduction within the surface is taken into account. The parameter $k \sim \frac{\alpha \lambda_s}{c_{ps} m_w}$ involving both the material and boundary layer properties is thus an important one in determining possible cross hatching on an ablation surface.

In conclusion, the present work suggests several areas for further investigation.

a. Extension of the viscous sublayer analysis to include the case where the mean flow profiles are nonlinear, i.e., when this sublayer no longer lies within the laminar sublayer of a turbulent boundary layer flow.

b. Improvement of the theoretical model of the ablating wall to include partial ablation conditions (ablative specie mass fraction significantly less than unity).

c. A comprehensive parametric study of the present heat transfer and ablative wall solutions over a range of $\alpha\delta_0$, Me and (especially) sweep angles ϕ to obtain specific numerical values of the resonance wavelength as a function of k .

d. Non-ablating wavy wall experiments in the case of a fixed surface temperature in which the heat transfer perturbations can be measured and compared with theory.

REFERENCES

1. FANNELÖP, T. & FLÜGGE-LOTZ, I. : The laminar compressible boundary layer along a wave-shaped wall.
Ing. Archiv, Band 33, Heft 1, p. 24-35, 1963.
2. BERTRAM, M.H., WEINSTEIN, L.M., CARY, A.M., ARRINGTON, J.P.: Heat transfer to wavy wall in hypersonic flow.
AIAA J. Vol. 5, No 10, pp 1760-1767, 1967.
3. MILES, J.W. & RODDEN, W.P.: On the supersonic flutter of two dimensional infinite panels.
J.Aero. Sc., vol. 26, 1959.
4. NACHTSCHEIM, P.R.: Analysis of the stability of a thin liquid film layer adjacent to a high speed gas stream.
NASA TN D-4976, 1969.
5. LARSON, H.K. & MATEER, G.G.: Cross-hatching - a coupling of gas dynamics with the ablation process.
AIAA Paper No 68-670, 1968.
6. WILLIAMS, E.P. & INGER, G.R.: Investigations of ablation surface cross-hatching.
SAMSO TR 70-246 (McDonnell Douglas Astronautics), June 1970.
7. LIGHTHILL, M.J.: Reflection at a laminar boundary layer of a weak steady disturbance to a supersonic stream, neglecting viscosity and heat conduction.
Quart. J. Mech. and appl. Math., vol. III, no 3, pp 302-325, 1950.
8. LIGHTHILL, M.J.: On boundary layers and upstream influence II. Supersonic flows without separation.
Proc. Royal Soc. A 217, pp 478-507, 1953.
9. BENJAMIN, T.B.: Shearing flow over a wavy boundary.
J. Fluid Mech., vol. 6, pp 161-205, 1959.
10. MILES, J.W.: On the generation of surface waves by shear flows.
J. Fluid Mech. vol. 3, p. 185, 1957.
11. LEES, L. & RESHOTKO, E.: Stability of the compressible laminar boundary layer.
J. Fluid Mech., vol. 12, No 4, pp 555-590, 1962.
12. BROWN, W.B.: Stability of compressible boundary layers.
AIAA J. vol. 5, No 10, pp 1753-1759, 1967.
13. INGER, G.R.: Discontinuous supersonic flow past an ablating wavy wall.
AIAA J., vol. 7, No 4, pp 762-764, 1969.

14. INGER, G.R.: Rotational inviscid supersonic flow past a wavy wall.
Bull. American Phys. Soc., vol. 13, p. 1579, 1968.
(APS Fluid Dyn. Div. Meeting, Seattle, Nov. 1968)
15. MARTELLUCCI, H., RIE, H. & SOMETOWSKI, J.F.: Evaluation of several eddy viscosity models through comparison with measurements in hypersonic flows.
AIAA Preprint 69-688.
16. LEW, H.G. & LI, H.: The role of the turbulent viscous sub-layer in the formation of surface patterns.
General Electric Miss. & space Div., Space Sci. Labs, R68SD12, 1 68.
17. NICHOLS, R.J. & SICHEL, M.: Thermal and ablative lag induced by a periodic heat input.
AIAA J. vol. 7, pp 139-144, Jan. 1969.
18. HOLSTEIN, H.: Über die aussere und innere Reibungsschicht bei Störungen laminarer Strömungen.
Z. angew. Math. u. Mech., Band 30, Heft 1/2, pp 25-49, 1950.
19. KLEIN, E.J.: Liquid crystals in aerodynamic testing.
Astronautics & Aeronautics, vol. 6, No 7, 1968.
20. McCLURE, J.D.: On perturbed boundary layer flows.
M.I.T. Fluid Dyn. Res. Lab. Rep. 62-2, 1962.
21. HOSOKAWA, I.: Transonic flow past a wavy wall.
Nat. Aeron. Lab. Japan, Tokyo, 1960.

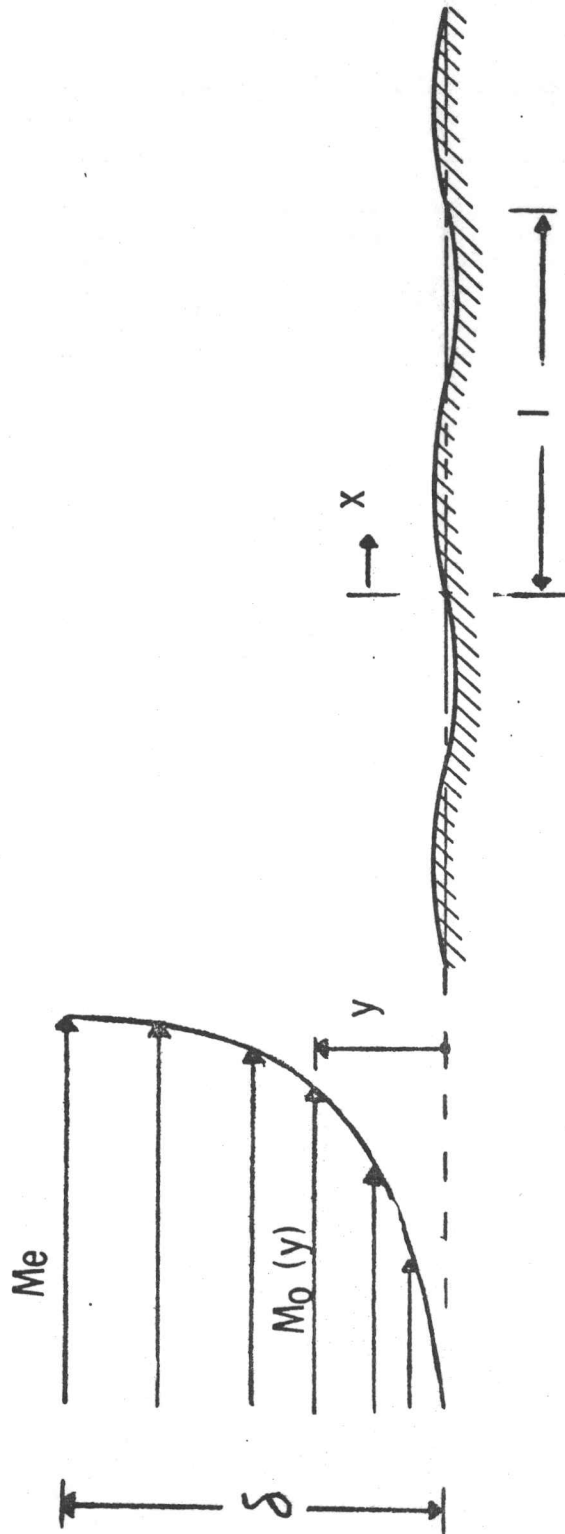


FIGURE 1 FLOW CONFIGURATION (SCHEMATIC)

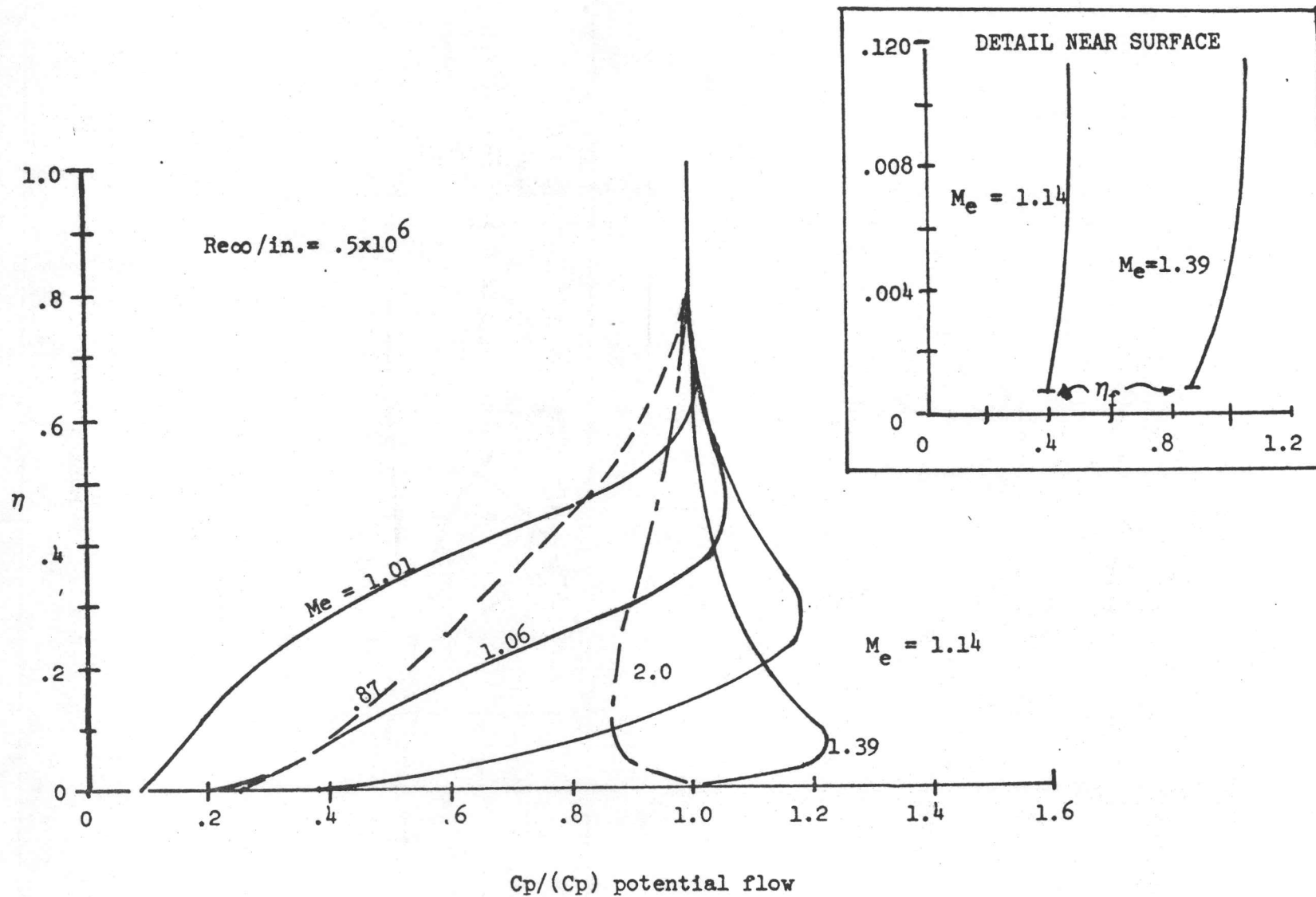


FIGURE 2. THEORETICALLY - PREDICTED PRESSURE AMPLITUDE VARIATION
 ACROSS A TURBULENT BOUNDARY LAYER

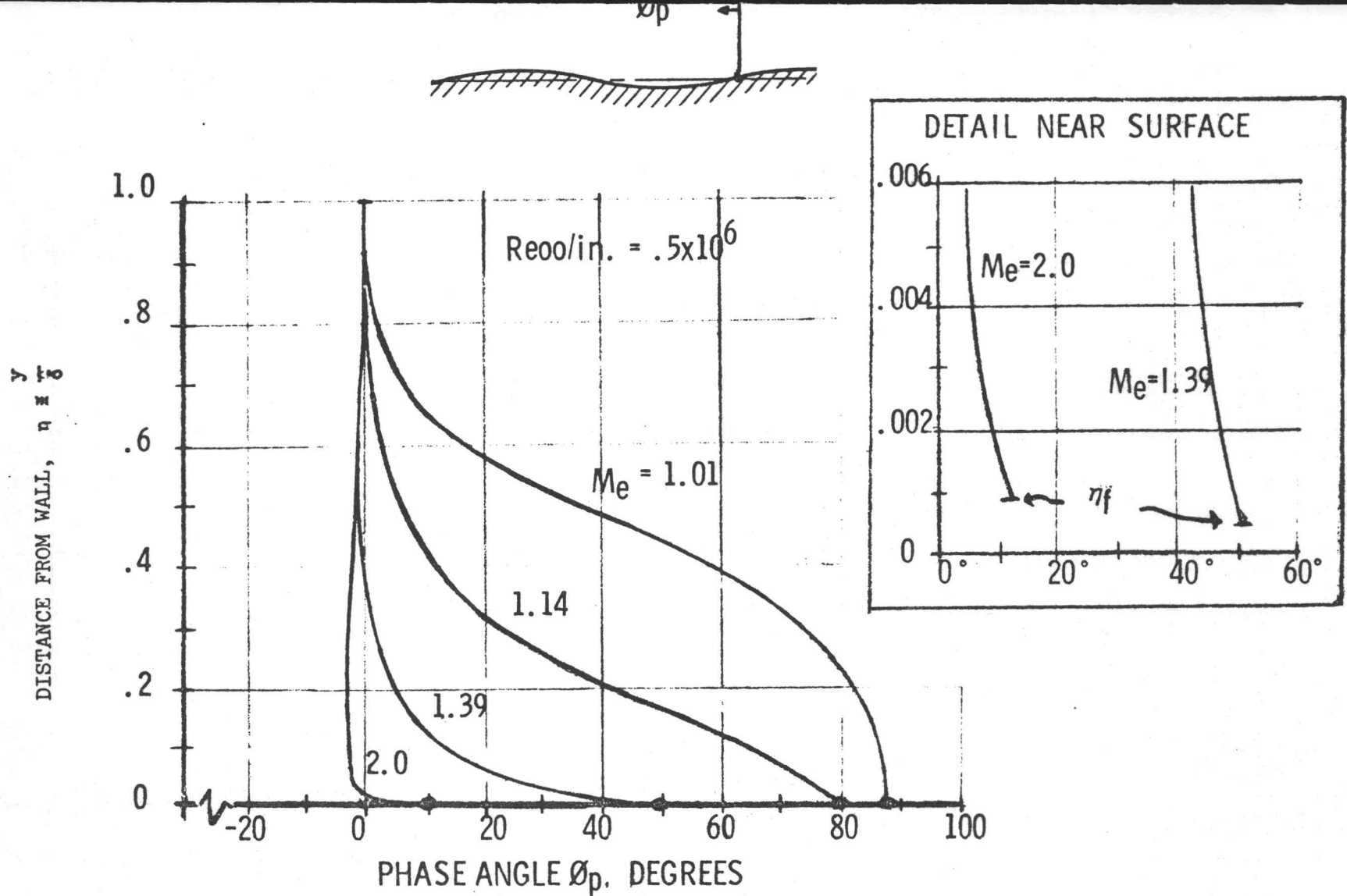


FIGURE 3. THEORETICALLY - PREDICTED PRESSURE PHASE ANGLE VARIATION
ACROSS A TURBULENT BOUNDARY LAYER

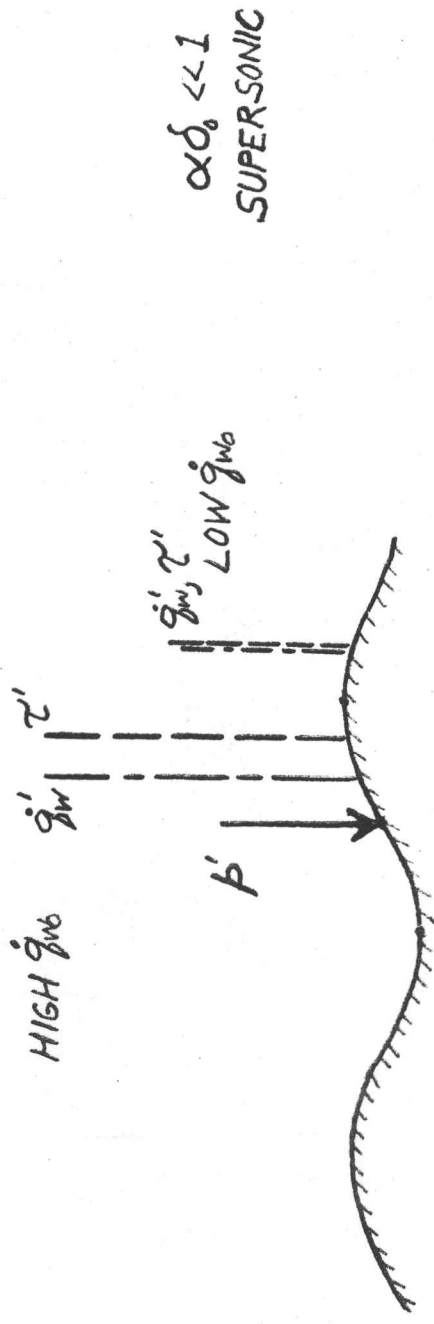
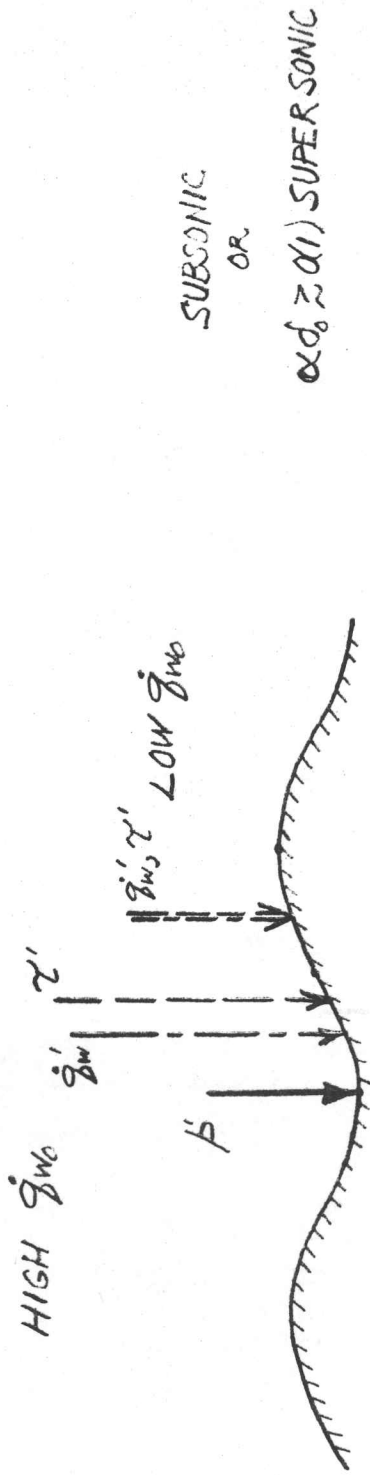


FIGURE 4. PHASE RELATIONS OF WALL PERTURBATION MAXIMA

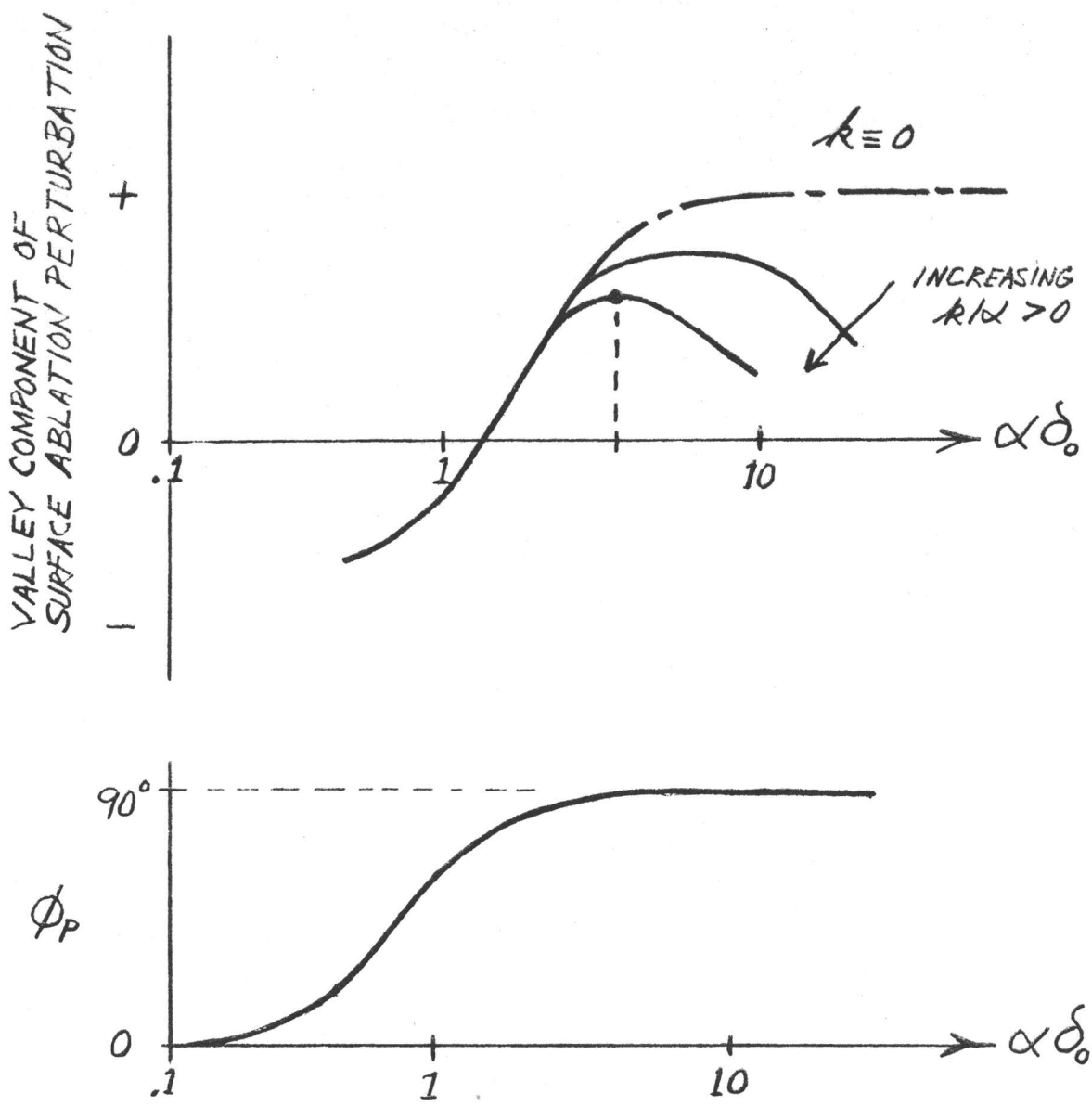


FIGURE 5. ILLUSTRATION OF STREAMWISE HEAT CONDUCTION EFFECT ON CRITICAL WAVELENGTH (SCHEMATIC)

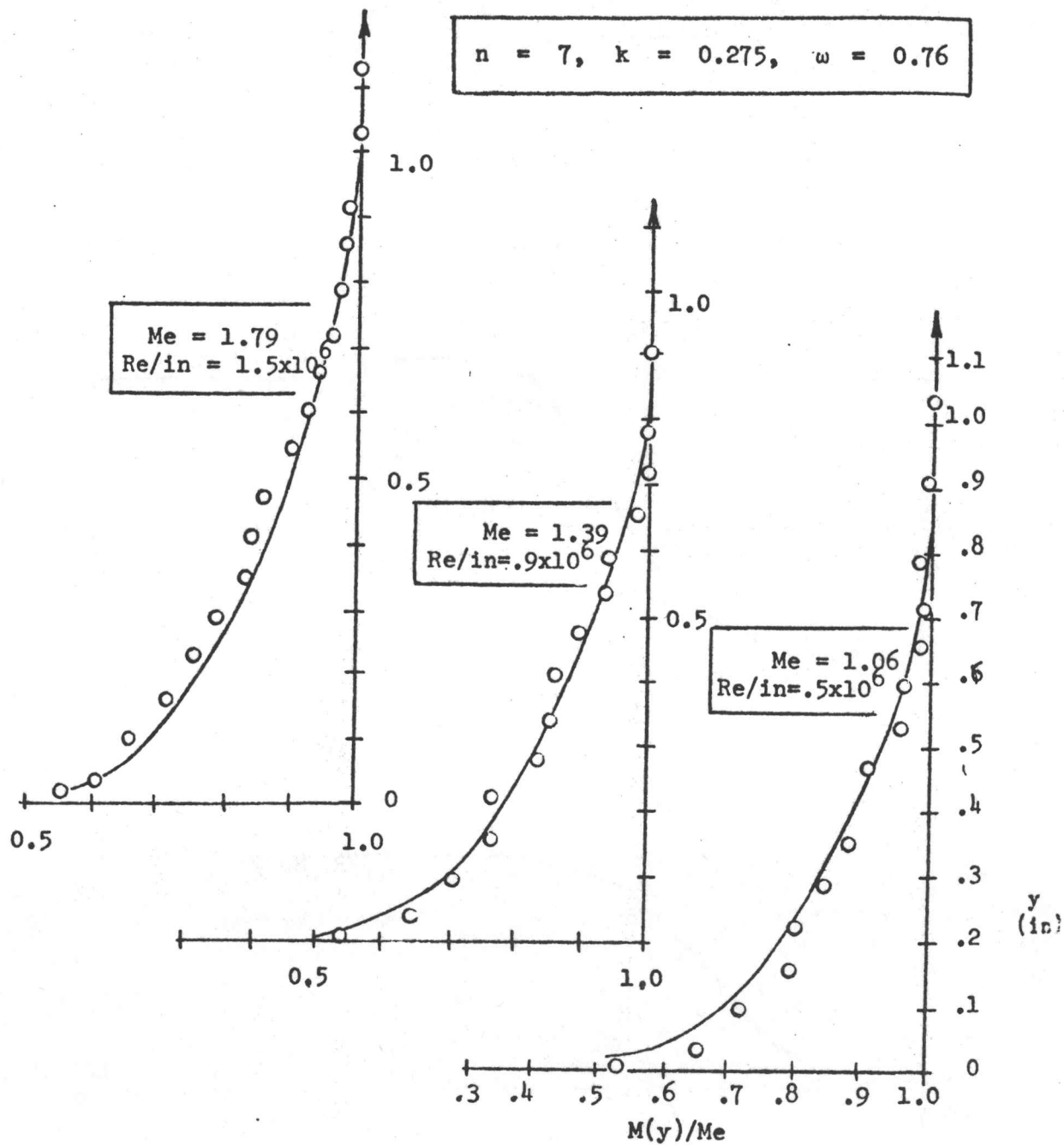


FIGURE 6. COMPARISON OF THEORETICAL AND EXPERIMENTAL BOUNDARY LAYER PROFILES

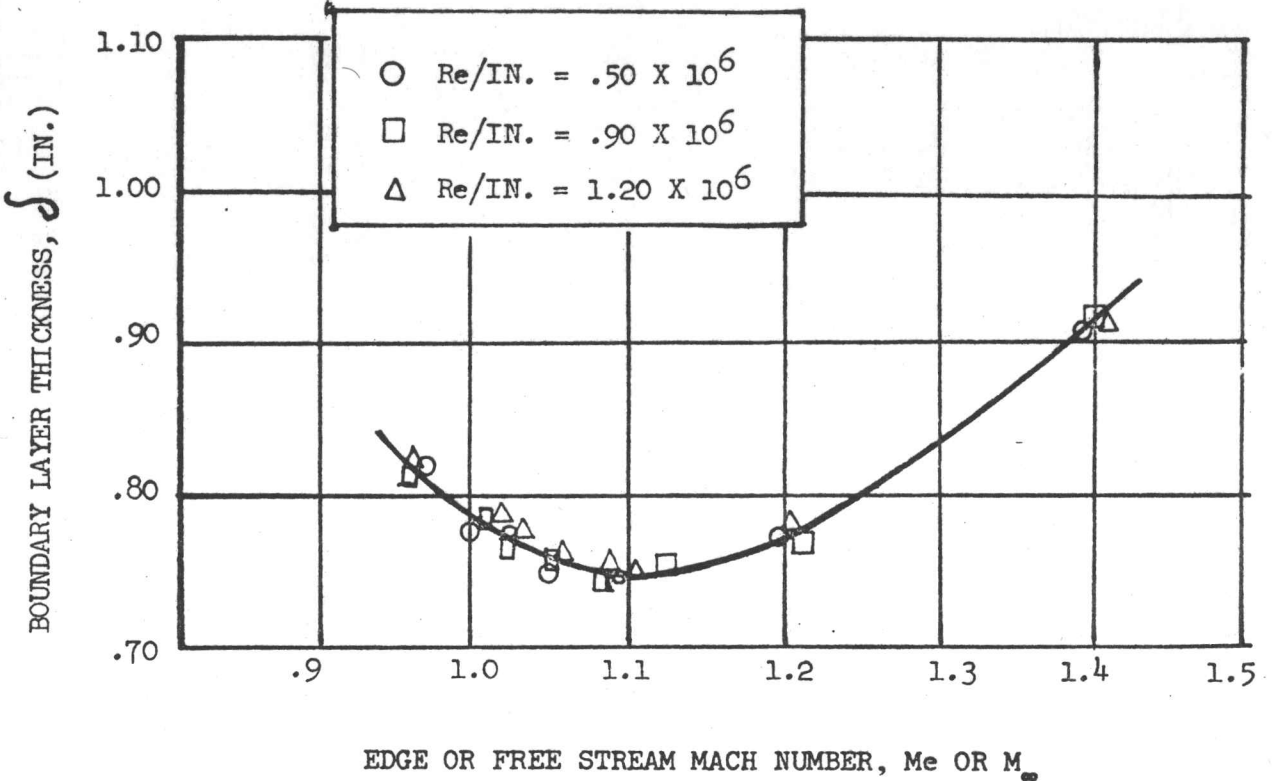


FIGURE 7. BOUNDARY LAYER THICKNESS

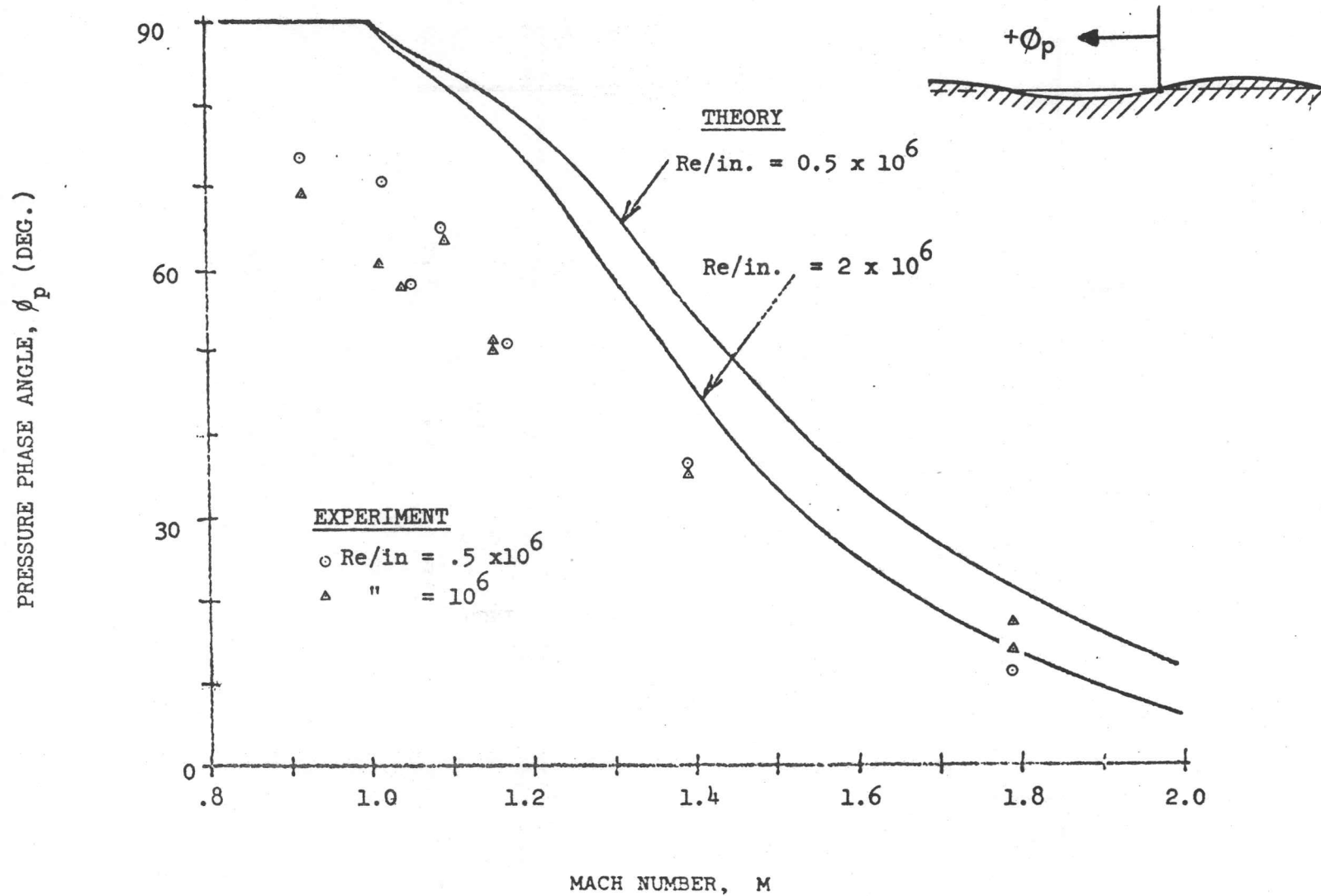


FIGURE 8. COMPARISON OF THEORETICAL AND EXPERIMENTAL PRESSURE PHASE ANGLE VARIATIONS WITH MACH NUMBER

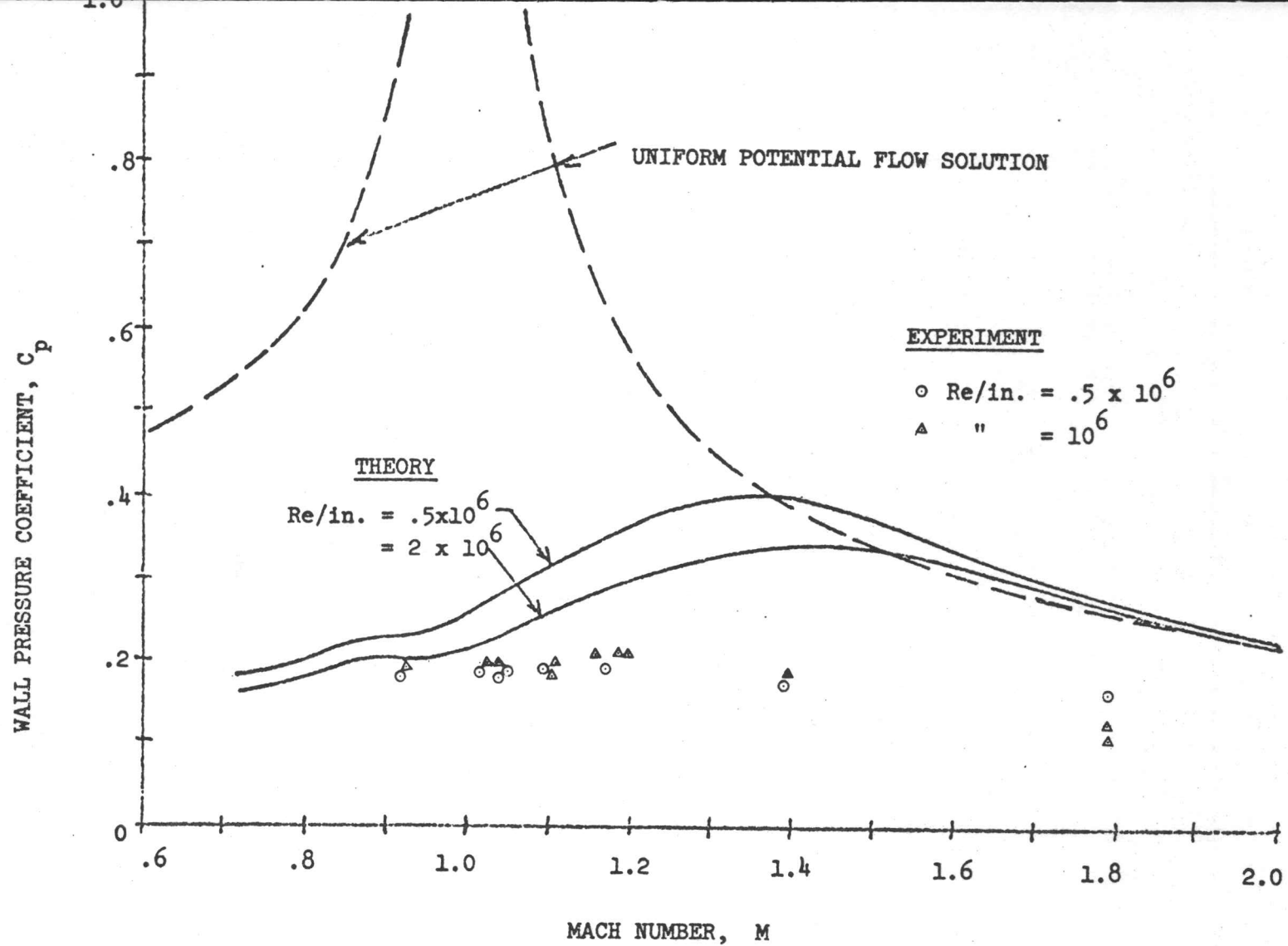
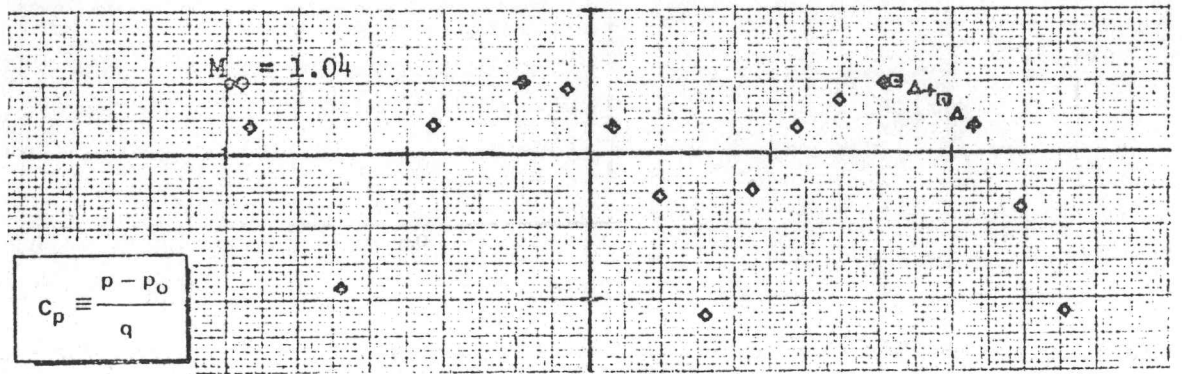
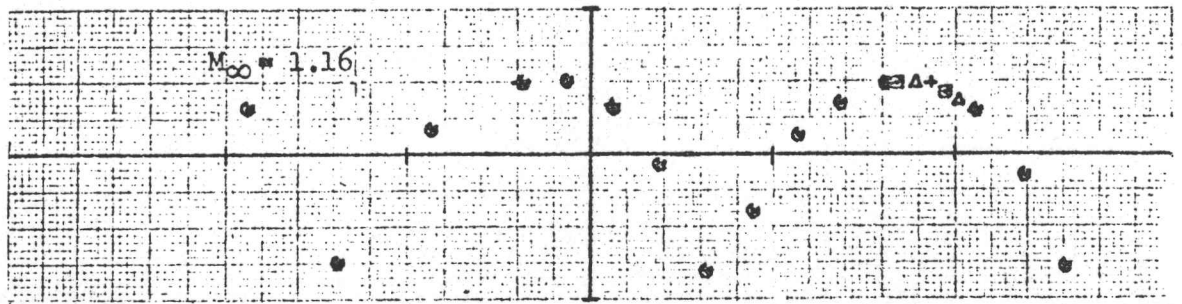
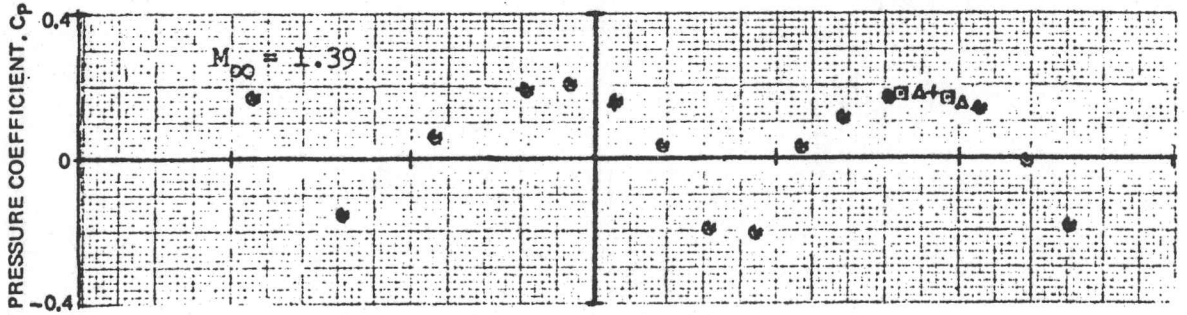
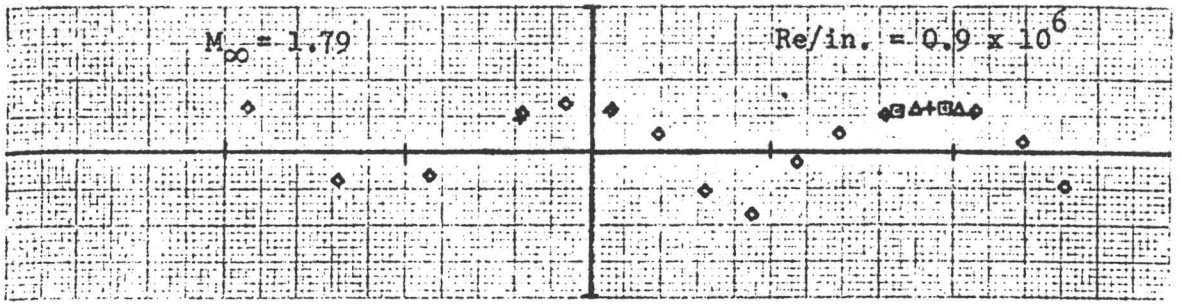


FIGURE 9. COMPARISON OF THEORETICAL AND EXPERIMENTAL WALL PRESSURE AMPLITUDES



$$C_p \equiv \frac{p - p_0}{q}$$

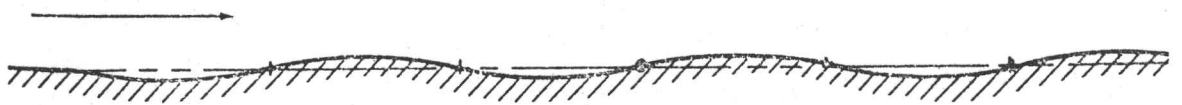


FIGURE 10. COMPARISON OF THEORETICAL AND EXPERIMENTAL WALL PRESSURE AMPLITUDES

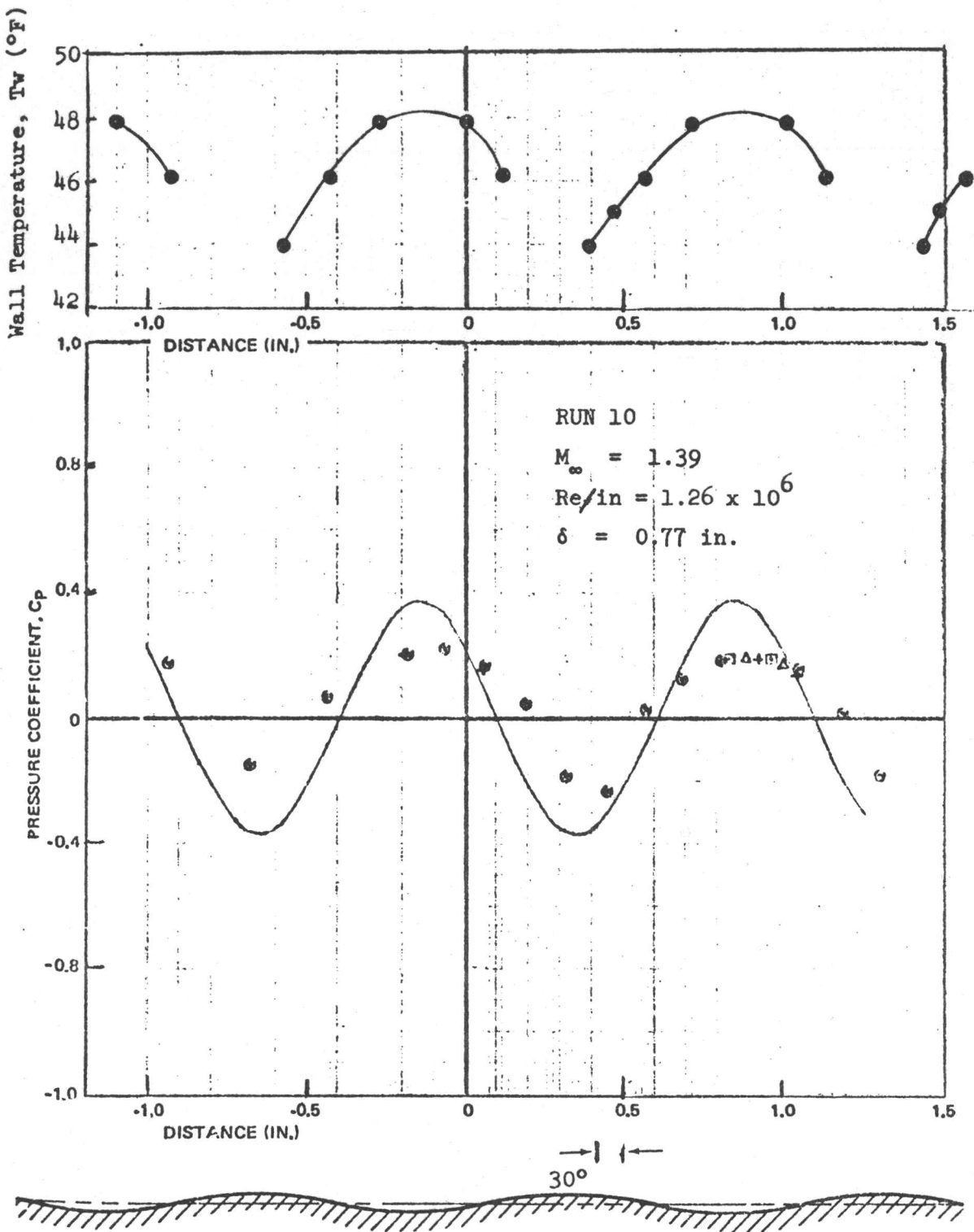


FIGURE 11. TYPICAL CORRELATION BETWEEN PRESSURE AND TEMPERATURE MEASUREMENTS